POLITECNICO DI MILANO

School of Civil, Environmental and Land Engineering

Master of Science in Environmental and Geomatic Engineering

Comparison and sensitivity analysis of marine CSEM exploration methods

Master Dissertation by

Babak Taleghani

Supervisor

Prof. Giancarlo Bernasconi

A. Y. 2015/2016

I

To my kindest parents, and to my dear uncle Abbas

Acknowledgement

I would first and foremost like to thank my supervisor, Prof. Giancarlo Bernasconi, who offered me such a great opportunity to study in the Applied Geophysics, Department of Electronic and information, Politecnico Di Milano. I am grateful to him for his assistance and his great ability to lucidly explain the most difficult concepts to me. I thank him for his time, his constant encouragement and for always enlightening the positive side of a situation. I deeply appreciate his full support for providing invaluable assistance that ultimately made this thesis a reality. With regards to research, he has always insisted that I try to find worthwhile questions to answer.

I would like to thank prof. Gentili for his generous help for introducing me to the world of Sensitivity analysis.

Of course, I must also express my gratitude to the entire Electronic and information Department of Politecnico Di Milano. In particular, I am grateful to Andrea Gola for all fruitful discussions we had.

Moreover, I would like to thank the many people from whom I learnt over the years; in particular, Prof. Dr. Toraj Mohammad and Eng. Mohammad Samei who taught me a great deal about looking at modelling process and interpreting data.

Also deserving special thanks to Ahmad Abedi, and my Uncle, Abbas Sanjari who were extremely kind and supportive during my study at Politecnico Di Milano. I would like to offer another special thanks to Sepehr Marzi for his full academic support.

I would like to express my gratitude to my parents who supported me over the years and encouraged me to keep going, I am forever indebted for their full kindest support in every single step of my life.

Table of Contents

List of Figures

List of Tables

Symbols and Notations

σ ……………………………. .. Bulk conductivity

$\emptyset$ ……………………………….. Porosity

μ ………………………………. Magnetic permeability

ε ……………………………… dielectric permittivity

ρ ……………………………… Density

ρ_r………………………….... Resistivity

J ……………………………… Matrix of Jacobean

MVO ……………………………. Magnitude vs. off-set

PVO ……………………………… Phase vs. Off-set

E ……………………………… Electric field intensity

B ……………………………… Magnetic flux density

τ ……………………………… Characteristic diffusion time

Abstract

Hydrocarbon deposits in the form of petroleum, natural gas, and natural gas hydrates occur offshore worldwide. Electromagnetic methods that measure the electrical resistivity of sediments can be used to map, assess, and monitor these resistive targets. In particular, quantitative assessment of hydrate content in marine deposits, which form within the upper few hundred meters of seafloor, is greatly facilitated by complementing conventional seismic methods with EM data.

In this study we developed comparison test between the acquisition configurations, VED, HED and TSEM one-dimensional reservoir response to the diffusive EM field.

This thesis explores the comparison and sensitivity analysis of Marine CSEM data with respect to the more important acquisition Configurations (VED, HED and TSEM), namely with different frequencies (0.2Hz, 0.48Hz, 0.76Hz, 1.04Hz) based on 1D – forward modeling. This analysis helps the interpreters to highlight the reliability of each acquisition method parameter in a complex CSEM inversion and gives them the idea to select the more efficient method for CSEM survey according to geometry of hydrocarbon deposit.

Keywords: Marine Controlled Source Electromagnetic (M-CSEM), Sensitivity Analysis, Forward modelling, Vertical electric dipole (VED), Horizontal electric dipole (HED), Towed source EM (TSEM)

Chapter 1   Introduction to Marine Controlled Source EM (CSEM) For Hydrocarbon Deposit Exploration

1.1   Brief Background of Hydrocarbon Deposit Exploration

Measurements of electrical resistivity beneath the seafloor have traditionally played a crucial role in hydrocarbon exploration (*Eidesmo, et al., 2002*). Electromagnetic (EM) sounding methods represent one of the few geo scientific techniques which can provide information about the current state and properties of the deep continental crust and upper mantle (*Boerner, 1992*). As the industry's search for hydrocarbon resources intensifies, more geoscientists are relying on these electromagnetic fields to probe areas that are difficult to image with seismic methods. The study of electrical currents in the Earth, called tellurics, is not new, first reported combining a measurement of electric and magnetic fields, termed magnetotellurics (MT), for exploration of the Earth's subsurface in 1952.2 However, MT has become an important tool for explorationists in the E&P industry only within the past few years—thanks to advances in 3D modeling and inversion technology. Now, MT results can be combined more efficiently with seismic and gravity surveys, resulting in a more calibrated model of the earth (*James Brady, et al. 2009*). At the start of the 21st century, the use of CSEM expanded from onshore mining exploration into new applications for hydrocarbon exploration, initially in deep water (500 m or more) and, more recently, in shallower water (less than 500 m). The basic idea behind the use of CSEM for hydrocarbons is to identify resistive layers in an otherwise conductive environment.

Charlie Cox, Professor of Geophysics at Scripps Institution of Oceanography, initiated and conducted the original academic research and developed early marine EM equipment some 25 years ago. The main focus of his work was in the field of crustal and deep ocean trench studies.

By 2000, Statoil and a major U.S. oil company (MUOC for short) were evaluating the CSEM method and its application in oil and gas exploration. Statoil had the first new CSEM survey performed offshore Angola, West Africa. The survey used existing Scripps receivers and Southampton's EM source and, although the data recorded were of relatively low resolution compared with the quality of data now being recorded 3.5 years later (10-13 against 10-15 today), the survey was a technical success. This effort proved that the CSEM method could be used for commercial oil exploration. Since then several major oil companies have invested significantly in appraisal and exploration application in this new technology and three service companies are now actively using and developing the technique in a variety of basins around the world (*Steven Constable and Leonard J. Srnka, 2007*).

1.2 Physical Properties and Behaviors

1.2.1 Geologic Properties

In order to discuss the nature of EM methods, it is useful to discuss the natural properties that affect the method. The property of interest is electrical conductivity and is related to the fluid-bearing rocks, here typically water saturated sedimentary units, through Archie's Law (*Archie, 1942*). The version of Archie's Law typically used in the hydrocarbon industry for brine and gas Filled sandstones:

$$\sigma = a\sigma_f S^n \emptyset^m$$

σ Is the bulk conductivity of the sample, a is tortuosity factor varying by rock type, S is the fraction of fluid (typically water) in the pores, σ_f conductivity of fluid, n is the water saturation coefficient along with m the cementation coefficient (both typically between 1 and 2), and $\emptyset$ is the porosity

(Volume fraction of pore space). Pores can be filled by various mixtures of fluids or even air. It can be seen that this equation is dependent only on _f and not on the conductivity of the rock mineral.

Therefore, the assumption is that the more conductive fluid (by order of magnitude) dominates the bulk conductivity.

A large factor affecting electrical properties is permeability, or how well the pores are connected.

This is represented by the cementation coefficient. A formation may have high porosity (large fraction of pore space), with low permeability, or vice versa. In hydrocarbon exploration, low permeability are typically found in sedimentary units with small grain sizes, such as shales.

In mineral exploration conductive veins, dykes, or even massive sulphide bodies of various geometries may be of interest, and may be more affected by joint and fracture sets over pore spaces.

Differences between maximum permeability and minimum permeability can also be modeled using

Hashin-Shtrikman bounds (*Hashin and Shtrikman, 1963*), in which a two-phase conductivity model of different pore geometries are used (max and min m values).

The ocean floor above hydrocarbon bearing formations typically consists of unconsolidated sediments of up to 60% porosities in which pore spaces are filled with seawater. The cementation coefficient for the same marine sediments are usually between 1.4-1.8. This

3

gives resistivity of 1-3Ωm. Hydrocarbon reservoirs typically have resistivity values one to two orders of magnitude higher depending on the nature of the reservoir. The resistivity of seawater varies with depth within the water column and can be measured during a survey, but a good overall average is 0.3 Ω m.

1.2.2 Petro physical Properties

In the framework of hydrocarbon exploration, several researches on rock physics are conducted by oil companies for improving their expertise on the characterization of the subsurface media. The rock physics allows us to investigate and to integrate the information carried by the several well log measurements. Following, will be introduced the rock properties (*Schön J.H. 1996*).

1.2.2.1 Porosity

Pores are local enlargements in a pore space system that provides most of the volume available for fluid storage. Porosity ϕ is defined as the ration of the volume of void or pore space Vp to the total or bulk volume of the solid matrix.

$$\emptyset = \frac{V_p}{V} = 1 - \frac{V_m}{V}$$

This quantity is dimensionless and is generally expressed as ratio or percentage. Porosity is the result of several geological, chemical and physical processes**.**

1.2.2.2 Saturation

Fluid saturation is the petro physical property that describes the amount of each fluid type, (oil, water or gas), V_f in the pore space. It is defined as the fraction of the pore space occupied by a fluid phase.

$$S_f = \frac{V_f}{V_p}$$

For a given specimen has to be verified that $S_{Oil} + S_{Water} + S_{Gas} = 1.0$ Fluid saturation can also be expressed in percentage.

1.3   Marine EM Theory

The theory here is based upon the development given in *Ward and Hohmann (1987)*. Electromagnetic fields are useful in geophysics due to their interactive nature with the medium through which they propagate *(Zhdanov 2009)*. This interaction can be used to determine certain physical properties of rocks, that is; electrical conductivity σ, dielectric permittivity ε, and magnetic permeability μ. For forward modeling problem, the operator equation is described by (*Zhdanov 2009*) as

$$\{E, H\} \cong A^{em}\{\varepsilon, \sigma, \mu\}$$

Where A^{em} is an operator of the forward electromagnetic problem (non-linear in general).The electromagnetic methods are based on the study of the propagation of electric currents and electromagnetic fields in the Earth. There are two methods that can be used;

- The direct current (D.C) methods or resistivity methods:- these considers injecting an electric current in the earth by a system of current electrodes and measuring the electrical potential with receiver electrodes; where, a low frequency current (<100 Hz) is used, to propagate inside the Earth practically like a direct current *(Zhdanov 2002).* The D.C surveys are used to determine the resistivity of the rocks. The resistivity of the rock provides information about the mineral content and the physical structures of rocks, and also about fluids in the rocks. However, D.C survey are limited by their failure to penetrate through resistive formations *(Zhdanov 2002).*
- Electromagnetic induction methods: these are based on transient field which overcomes the limitation above since transient fields easily propagates through resistors. This method in addition to resistivity provides information about magnetic permeability μ, and dielectric constant ε. *Zhdanov (2002)* indicates that this method can be used for ground, airborne, sea bottom and borehole observations. In this type, the receivers measures the total field formed by the primary signal in the transmitter and a scattered signal from the internal structures of the Earth.

1.3.2   Amplitude and Phase

The amplitude of the secondary field is measured usually by expressing it as a percentage of the theoretical primary field at the receiver or as the resultant of the in-line and the cross-line fields. Phase shift and the time delay in the received field by a fraction of the period, can also be measured and displayed. The second method of presentation of the field is to electronically separate the received field into two components; (1) In-phase (the

"real") and, (2) Out-of-phase (the "quadrature" or "imaginary") component with the transmitted field.

In frequency domain electromagnetics, depth and size of the conductor primarily affect the amplitude of the secondary field. The quality of the conductor mainly affects the ratio of in phase to out-of-phase amplitudes.

The presence of the resistive layer results in an increased amplitude and less phase lag for both the inline and vertical components, as expected since in the resistive reservoir there is much less attenuation and phase shift of the diffusing energy than in the conductive sediments *(Kerry Key , 2011).*

1.3.3   Skin Depth and Penetration

The attenuation constant (skin depth) defines the rate of decay of the wave fields as the waves propagate. Skin depth is the distance over which a plane wave is attenuated by a factor of e^{-1} in a good conductor, or as the depth at which flux density and eddy currents have decayed to e^{-1} of their surface value. Thus the decay from the surface to the interior is exponential.

$$E(X) = E_0 e^{-\alpha x}$$

$$E(\delta) = E_0 e^{-\alpha \delta}$$

$$E(\delta) = E_0 e^{-1}$$

Thus $\alpha \delta = 1$

And from (*Constable 2010*), it then follows from equations above that

$$\delta = \frac{1}{\alpha} = \frac{1}{\sqrt{\pi f \mu \sigma}}$$

With f is the frequency (Hz), σ is the electrical conductivity (S/m), and μ is absolute magnetic permeability of the conductor. Due to the skin depth effect, very low frequencies (0.05-1 Hz) are applied (*S. E. Johansen, H.E.F. Amundsen et al. 2005*), if a deep sub-seafloor target must be penetrated. The antenna frequency affects the resolution on the E-field contrast when evaluating models with and models without hydrocarbon. The relationship between

any frequency and the maximum depth of detectable reservoirs (*Tadiwa, Yahya et al. 2013*) can be given by

$$Z_{max} = 600 - 851.2\ln(f)$$

Where, Z_{max} the maximum depth, and f is the antenna frequency. EM signals are rapidly attenuated in seawater (approximately 551m at 0.3 Ω-m) and seafloor sediments saturated with saline water. These signal pathways will dominate at near source-to-receiver offsets (approximately 3km) (*S. E. Johansen, H.E.F. Amundsen et al. 2005*).

The magnitude of the external electromagnetic noise decreases with depth, because of the skin depth effect that dampens high frequencies. Hence, the signal-to-noise ratio usually increases with water depth (*Terje Holten el, al., 2009*)

In the frequency domain, however, the longer skin depths associated with seafloor rocks mean that at a sufficient source-receiver distance, the field is dominated by energy propagating through the geologic formations. Energy propagating through the seawater has essentially been absorbed and is absent from the signals. Furthermore, by concentrating all the transmitter power into one frequency, larger signal-to-noise ratios can be achieved at larger source-receiver offsets *Constable, S. and L. Srnka* (2007).

1.4   Marine Controlled Source EM in Practice

Controlled source EM application, an electric dipole transmitter system is deep-towed from a ship and passes a time-varying current (typically 500–1,000 A) between electrodes spaced apart by some distance (typically 100–300 m), producing an electromagnetic field that diffuses through the ocean, seafloor and air. As the EM field diffuses away from the transmitter, it is modified by the conductivity of the media it passes through. The resulting attenuation and phase shift of the transmitted EM field is recorded by an array of seafloor EM receivers containing electric field sensing dipoles and induction-coil magnetometers. Typical receivers for the 0.1–10 Hz bandwidth of most CSEM applications are based on AC - coupled electric field sensors and induction-coil magnetometers of similar design to the instrument described in *Constable et al. (1998).*

Marine CSEM was first used to measure the conductivity of the lithosphere (*Cox 1981*), while other early academic applications largely focused on detecting conductive magma chambers and hydrothermal systems at mid-ocean ridges (*e.g., Young and Cox 1981; Evans et al. 1991; Sinha et al. 1998; Mac Gregor et al. 2001)*. Only in the past decade has it become widely recognized that the CSEM method is sensitive to thin resistive hydrocarbon reservoirs trapped in conductive sediments on the continental shelves (*e.g., Edwards 2005; Constable and Weiss 2006; Um and Alumbaugh*

2007). The first industrial field trials were carried out a decade ago using existing academic receiver and transmitter technologies to effectively detect the EM signature of a large reservoir offshore Angola (*Ellingsrud et al. 2002; Eidesmo et al. 2002*). Subsequently, the method was incorporated into the offshore hydrocarbon exploration toolkit in the course of only a few years *(Constable 2010*).

Figure 1. Schematic representation of the horizontal electric dipole-dipole marine CSEM method

The geometry in this study will be considered as an azimuth of zero-degree. Presence of a hydrocarbon causes a decrease in electrical conductivity which gives it a unique character to be easily detected. In the view point with (*Eidesmo, S. Ellingsrud et al. 2002, Summerfield, Gale et al. 2005, Constable and Srnka 2007, Zhdanov 2009*), the survey geometry is considered to consist of electric receivers that are placed stationary by the concrete anchors on the seabed (figure 2.). The survey design determines how well the target can be detected and characterized.

Figure 2. The geometry of CSEM dipole fields. Along the polar axis of the dipole transmitter, the field is purely radial. Along the equatorial axis, the field is purely azimuthal. At other azimuths the received fields are a trigonometric mix of both modes (Constable and Weiss 2006).

1.4.1 Off-shore Scenario

The Marine CSEM method is particularly useful for detecting the first few percentage increases in hydrocarbon saturation at the edges of the reservoir. The electric anomalies represented by oil and gas reservoirs, which perturb the transmitted electromagnetic field, can therefore be detected in the survey data. The main goal is to determine and characterize possible thin resistive layers within the conductive surroundings beneath the seabed.

With marine CSEM now available and proven in principle, oil companies can use rock property data from well logging in appraisal, production and exploration to better understand and delineate the hydrocarbon-saturated reservoir section to which CSEM is most sensitive.

1.4.1.1 Transmitters

In the Most Marine CSEM acquisition nowadays uses a horizontal electric dipole (HED) source towed near the seabed and array of receiver dipoles on the seabed. The transmitter dipole emits a low frequency electromagnetic signal that propagates into the seawater column and downward into the subsurface (*Dell'Aversana, 2007*). A horizontal electric dipole,

is towed for several hundred meters, close to the seafloor to maximize the energy that couples to seafloor rocks *(e.g., Edwards, 2005)*.

Some details on the CSEM transmitter:

- The streamer can be up to 300 meters long
- Electric power is transmitted to the tow vehicle along the tow cable at high voltage,
- The voltage is reduced and current increased by a transformer at the tow vehicle, and a current of up to 1000 [A] is injected into the seawater.

Although other source con-figurations have been used, such as vertical electric dipoles (VED) sources that transmit a transient electromagnetic signal when the source is turned on *(Jon-Mattis Børven el, al. 2009)*.

VED antenna consists of two large electrodes connected to the vessel by heavy cables, The EM field is generated by sending a DC current through the lower electrode, which sits on the seabed during signal transmission, through the conductive seawater and back to the upper electrode. This electrode is lowered 30–50 m below the sea surface to minimize the influence on the EM field of the conductive hull of the survey vessel, while maximizing the transmitter dipole moment which is directly proportional to the strength of the transmitted EM field, the source signal consists of a series of pulses, each with a typical duration of 2–8s *(Jon-Mattis Børven el, al. 2009)*.Figure 3.
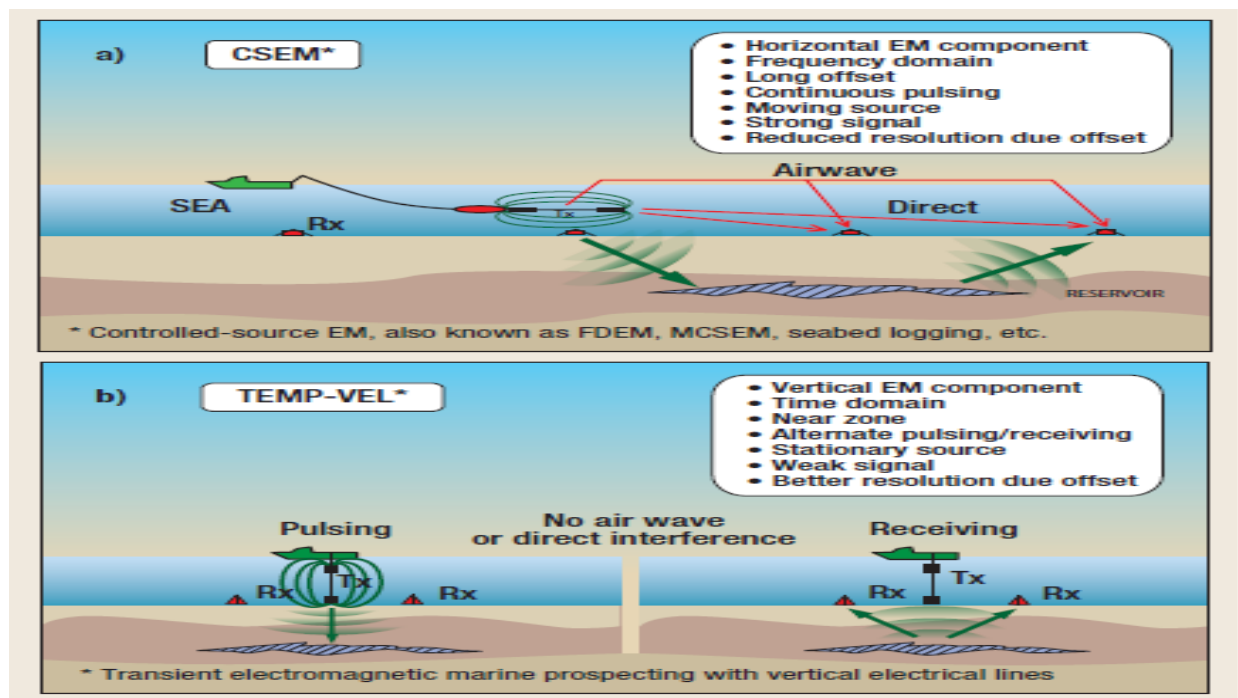
Figure 3. Overview of (a) conventional horizontal-based frequency domain, CSEM, such as SBL, and (b) the recent vertical-based time domain EM method. Note the acquisition setup and diffusion paths of the transmitted and recorded signals for the two methods.

1.4.1.2 Receivers

The EM receivers are autonomous sea floor units deployed at pre-determined locations. Receivers are equipped with magnetic as well as electric sensors which are oriented as the three spatial coordinates, Depending on the followed approach, time or frequency domain, record the time-varying source signal over source-receiver ranges from zero to several tens of kilometers, depending upon source waveform period and the conductivity below the seafloor, receivers provide respectively the transient or magnitude and phase of the received signal over the transmitter-receiver separation, offset (*P.J. Summerfield, el. Al., 2005*).

Receivers located at a suitable offset (distance between transmitter and receiver) range record the amplitude and phase of the horizontal electric field components. The appropriate offset range is typically 6–10 km *(Jon-Mattis Børven el, al. 2009).*

1.4.2 Field Penetration

Performing a marine surveying for hydrocarbon, it is very important to estimate the penetration of the electromagnetic field, into the sub-seafloor. Here, the skin effect describes the penetration of electromagnetic fields into materials.

We remind the well-known formula:

$$\delta = \sqrt{\frac{2}{\mu\omega\sigma}} \approx 500\sqrt{\frac{\rho}{f}}$$

Where δ is the distance, measured in meters, at which E and H fields are both attenuate by a factor e. This result is derived from the analysis of the wave equation in frequency domain. The same result can be obtained by performing the analysis in time domain, *(Nabighian M.N. el. Al. 1991). (Bostick, 1977),* introduces the equivalent depth of investigation of a plane wave which is derived from asymptotic relations based on a uniformly layered half-space. The result allows to get a rough calculation of the effective depth of investigation penetration D, measured in meters, of a plane wave in a medium:

$$D = \frac{\delta}{\sqrt{2}}$$

The electromagnetic wave propagation through the sub-seafloor, is facilitated by the particular geometry and electrical properties of the offshore scenario. The following considerations explain schematically the propagation phenomenon:

- Sea water has a skin depth bigger than distance dipole seafloor, few ten of meters, (Figure 4.1). This allows fields to diffuse through the sub-seafloor, for several thousand of meters, since the skin depth of the sub-seafloor is twice;
- The water column is larger than its skin depth, preventing the birth of airwave;
- For the previous reason, MT sources coming from the atmosphere do not reach the receivers;
- The first offset of the receiver line is widely bigger than water skin depth to prevent that direct fields reach the first receiver *(Fabio Marco Miotti, 2012)*.

1.4.3 Resolution

Due to the low frequency used in CSEM data acquisition, the vertical resolution is poor and will limit the ability to identify the thickness of the reservoir and the possibility of several stacked targets being present. Depending on the grid resolution and inversion/ migration algorithms used, there may be restrictions to mapping lateral extent *(Jonny Hesthammer, et. Al. 2010).*

It is important to cover sufficiently broad frequency range in order to improve the depth resolution. The spatial resolution of the EM data is mainly limited by the noise level and receiver spacing. it is challenging to reach depths of more than 3 km below the seabed due to lower resolution and the noise level becoming higher than the real signal *(Jonny Hesthammer, et. Al. 2010).*

The spatial resolution of CSEM method is lower compared to seismic since extremely low frequency are involved. The resolution is determined by the intrinsic characteristic of the diffusion equation which governs the electromagnetic phenomenon of CSEM technique. However, to perform a quantitative measure of CSEM resolution is quite complicated because considerable confusion exists on this topic, *(Constable, 2010. Constable S. and Srnka L.K. 2007).*

We start with the damped wave equation used to describe the vector electric field E in ground-penetrating radar:

$$\nabla^2 E = \mu\sigma\frac{\partial E}{\partial t} + \mu\epsilon\frac{\partial^2 E}{\partial t^2}$$

Where t is time, σ is conductivity (between 100 and 10^-6 S/min typical rocks), μ is magnetic permeability (usually taken to be the free space value of $4\pi *10^{-7}$ H/m in rocks lacking a large magnetite content), and ϵ is electric permittivity (between 10^{-9} and 10^{-11} F/m, depending on water content). The first term is the loss term, and disappears in free space and the atmosphere where σ = 0, leaving the lossless wave equation that will be familiar to seismologists *(Constable, 2010)*.

The vertical resolution of wave propagation is proportional to inverse wavelength, and a wave carries information accumulated along its entire ray path. Thus, as long as geometric spreading and attenuation do not prevent detection, a seismic wave carries similar resolution at depth as it does near the surface.

In the diffusion equation, the concept of resolution changes drastically. For a harmonic excitation, the entire medium composed by Earth Sea and air is excited by EM energy, and what is measured at the receiver is, in first approximation, the average of the whole system weighted by the sensitivity to each part of the system, which decreases with increasing distance from the observer. A reasonable definition of CSEM resolution, coming from the analysis of real data

(Constable, 2010), estimates the lateral and vertical resolution as the 5% of the depth of burial. At frequency 0 the previous diffusion equation reduces to the Laplace equation:

So resistive layers appear to be relatively independent from resistivity contrast. From analyses with real data can be assumed that resistivity variations have uncertainty around 10% of the obtained value. Further, EM methods appear to be more sensitive to conductive layers than resistive ones. This characteristic suggests we can discriminate with more resolution conductive target, while we cannot distinguish strong resistive layers from weak ones. Horizontal resolution depends mainly from the electric dipole dimension. As general rule, horizontal resolution corresponds, roughly, to the length of electric dipole.

This approximation is particularly true in TM propagation, *(Zonge, K. L. and Hughes L.J. 1991.).* From this property we have that, increasing the dipole length we lose resolution in favor of a deeper field diffusion, because we increase the power of radiation pattern. In opposite, decreasing the dipole length, we increase the resolution, but losing contemporarily efficiency on sub-seafloor penetration, (increasing the background noise). Finally, the resolution of the CSEM method also depends on the configuration of the transmitter-receivers system, as explained by the scheme introduced by *(Constable, 2010)*.

1.4.4 Data Acquisition

All CSEM methods utilize an active, or man-made, ac electromagnetic transmitter source to induce a secondary current in the subsurface and are attractive compliment or alternative to so-called "passive-source" electromagnetic methods such as magneto-telluric which rely on naturally occurring electromagnetic fields *(C. M. Swift 1991).* The CSEM exploration involves two different approaches for processing the collecting data: FD-CSEM, Frequency Domain Controlled Source Electromagnetic, and TD-CSEM, Time Domain Controlled Source Electromagnetic. Both are based on the same principle of the electromagnetic induction. The choice depends mainly from operational motivations. Following, both methods will be explained *(Edwards, 2005).*

1.4.4.1 Time Domain EM

In time domain CSEM, a large transmitter loop is laid out on the ground and most commonly a square-wave current is run through it. When the current abruptly goes to zero, in accordance with faraday's law, a short-duration voltage pulse is induced in the ground, which causes a loop of secondary current to flow in the immediate vicinity of the transmitter wire. These secondary currents in turn creates secondary magnetic and electric fields as they propagate and decay. Receivers placed some distance away from the source record various components of the electromagnetic fields produced.

The Time Domain CSEM technique involves as source a square wave form or pseudo random sequences (to select just only particular frequencies), for energizing the sub-seafloor. Effectively, the ground is energizing by passing an alternating current in a grounded loop which sustains a magnetic field. The energization is enabled every time on window, having length between 10µs – 10ms, Figure 4.
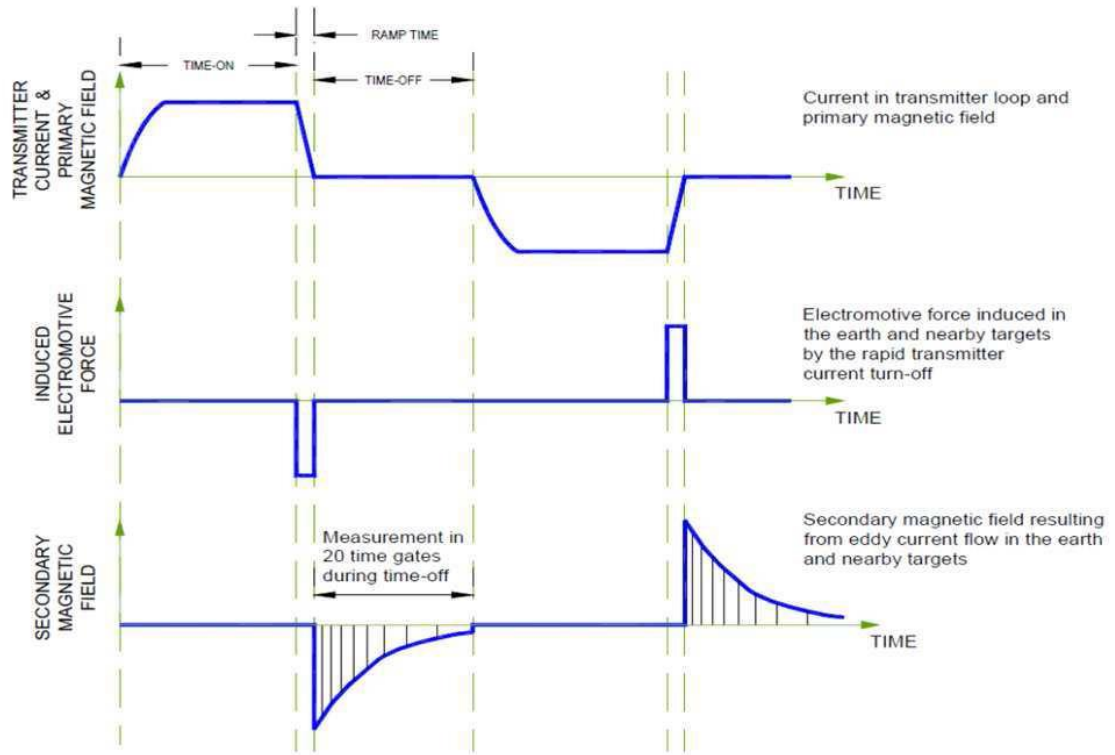
Figure 4. Time Domain CSEM - Electric field Transient

Electromagnetic induction causes the birth of eddy currents, which tend to propagate in the sub-seafloor for tens to hundred meters depending on the skin depth of the composite medium. At the end of each transmission time, Time off, receivers start to collect data. Stored data are turn-off transients associated to the electromagnetic fields backscattered by the sub-seafloor. To notice that, the entire procedure is performed at discrete time. As general rule, for every turn off transient, 20–30 intervals are considered. The stored transient are then added up together to obtain the final measure. This procedure, called stack as in seismic, allows to improve the SNR. We observe that the transmitter current, at the end of each time window, changes its phase of $\pm\pi$. This reduces the effects of local electromagnetic interferences, data polarization. To notice the decreasing/increasing turn off transient of the transmitter current, which produces an induced electromotive force in the heart and nearby targets, with the same frequency of the transmitted signal. At the end of each time off the signal tends to reach the self-potential value, determined by the particular chemical composition of the sub-seafloor. The TD CSEM allows to calculate the apparent resistivity of the sub-seafloor, in analogy with the geo-electric methods (DC methods). Since transients varies slowly, for obtaining the apparent resistivity measures is necessary to wait long transient before to obtain a stable signal (late stage) as indicated by *(Spies, 1991)*, who provides asymptotic relations, early and late stage, suitable for the calculation of the apparent resistivity in homogeneous layered half space. The receivers

acquire the transients *[ex(t), ey(t), ez(t)]* for the electric field and *[hx(t), hy(t), hz(t)]* for the magnetic field. The turn off velocity of the transient depends on the conductivity of the medium. The higher is the conductivity of the medium slower is the related transient.

1.4.4.2   Frequency Domain EM

The FD CSEM, is governed by the principle of electromagnetic induction. However some operational differences characterize this technique, in particular:

- The bandwidth of the source is very narrow compared to TD CSEM, in fact, theoretically FD CSEM involves pure sinusoid. It is evident the disadvantage of repeating the survey for collecting data at different frequencies,
- Data are collecting while the source energizes the sediment. Consequently, this technique requires the measurement of small secondary fields due to current flowing in the ground at presence of large primary fields generated by the source.

The marine electromagnetic exploration for finding hydrocarbons involves more frequently the FD-CSEM instead of TD CSEM, the source is affected by the continuous wave motion of the sea. Cause of wave motion, noisy data are stored and consequently also the stack will not have a high SNR. TD-CSEM is more suitable for land exploration since the source is motionless.

There are various transmitter waveforms available for frequency-domain CSEM, as it has been the method of choice since the commercial development of marine EM exploration. The choice of a waveform is dependent on the nature of the geology, particularly taking into account the skin depth of the host material in order to be sensitive to the exploration target. The simplest waveform is a periodic square wave in which the odd harmonics fall o in amplitude as 1=n and has been 38 utilized by both methods *(Fabio Marco Miotti, 2012)*.

1.4.5   Marine CSEM techniques

With the success of the controlled source electromagnetic (CSEM) technique in onshore mining exploration, the technique was expanded into new applications for hydrocarbon exploration, initially in deep water (500 meters or more) and more recently, in shallower water less than 500 meters *(Peace et al., 2004)*. The application of controlled source electromagnetic (CSEM) technique in offshore and marine environment is termed marine controlled source electromagnetic (mCSEM) or seabed logging as commonly used in the industry. The basic idea behind the use of controlled source electromagnetic (CSEM) for offshore hydrocarbon exploration is to identify resistive layers in an otherwise conductive environment *(J. Brady et al., 2009)*. The new marine controlled source electromagnetic

(mCSEM) method, although superficially similar to magnetotelluric, is different and uses an artificial electric dipole energy source instead of recording passive earth energy. This improves the resolution of the method by about an order of magnitude and permits the identification of thin, high-value resistors in a background matrix of low-resistivity conductor rock, down to tens of meters rather than the hundreds of meters typical of passive marine magnetotelluric resolution. With offset information from, for example, a nearby discovery well, the marine controlled source electromagnetic method can identify a target hydrocarbon-bearing reservoir rock in a structure before it is drilled *(Peace et al., 2004).* However, there are several methodological limitations regarding both acquisition operation and interpretation approaches *(P. Dell'Aversana 2010).*

1.4.5.1.   Acquisition Methods
1.4.5.1.1.   Horizontal Electric Dipole (HED)

Figure 5. Introduces the basic method we discuss. A horizontal electric-field transmitter is towed close to the seafloor to maximize the energy that couples to seafloor rocks. Although other source con -figurations have been used, such as vertical electric and horizontal magnetic dipoles e.g*., (Edwards, 2005),* the long horizontal electric dipole offers a number of practical and theoretical advantages; hence, it is the only source currently used in the industry. A series of seafloor electromagnetic receivers spaced at various ranges from the transmitter record the time-varying source signal over source-receiver ranges from zero to several tens of kilometers, depending upon source waveform period and the conductivity below the seafloor. Data processing — including time-domain stacking, Fourier transformation, and merging with navigation and position—converts these recordings into amplitude and phase of the transmitted signal as a function of source-receiver offset and frequency (which is typically between 0.1 and 10 Hz).
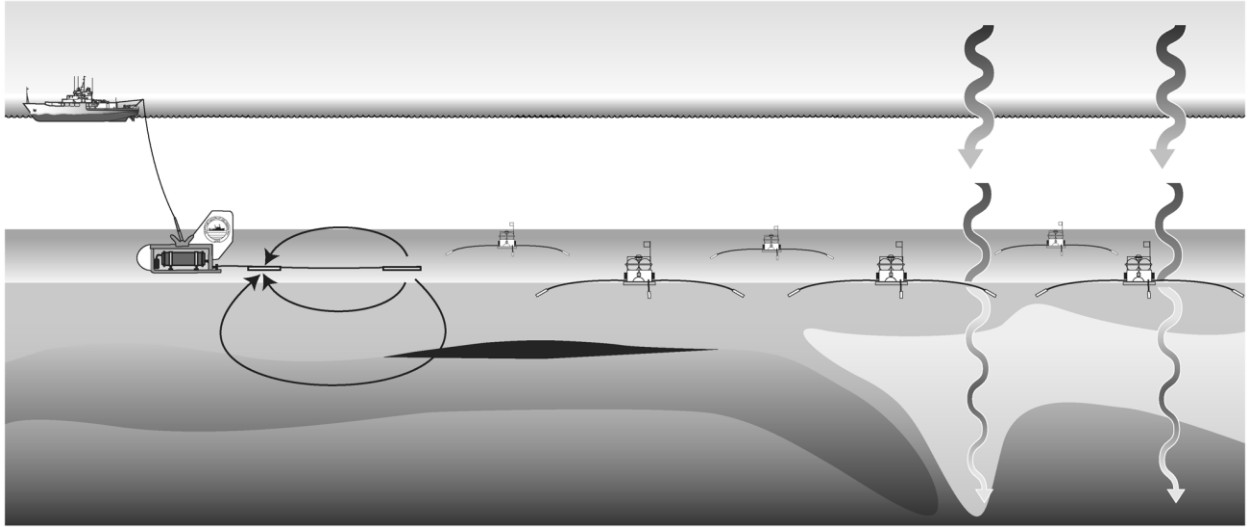
Figure 5. Schematic representation of the horizontal electric dipole-dipole marine CSEM method. An electromagnetic transmitter is towed close to the seafloor to maximize the coupling of electric and magnetic fields with seafloor rocks. These fields are recorded by instruments deployed on the seafloor at some distance from the transmitter. Seafloor instruments are also able to record magnetotelluric fields that have propagated downward through the seawater layer

In geophysics, electric and electromagnetic EM methods are used to measure the electric properties of geologic formations. At the low frequencies used in marine CSEM, rock resistivity accounts for almost all of the electromagnetic response. Because replacement of saline pore fluids by hydrocarbons gas, gas condensate, or oil increases the resistivity of reservoir rocks, EM methods are clearly important exploration tools.

1.4.5.1.2　　Vertical Electric Dipole (VED)

Recently, a new TCSEM method using a vertical electric dipole (VED) source has been developed *(Holten et al., 2009; Flekkoy et al., 2010)* Unlike the conventional TDCSEM method described above, the new TDCSEM method with the VED source utilizes relatively short source-receiver offsets (e.g., 500 to 1500 m). The transient currents originating from the lower tip of the VED source diffuse directly downward to the seabed. The currents interact with a resistive structure (e.g., hydrocarbon reservoirs) below the source. The resulting anomalous EM fields are measured at short offsets and are utilized to interpret deep seabed structures. Modeling studies of the TDCSEM method with the VED source have been recently presented *(Scholl and Edwards, 2007; Alumbaugh et al., 2010; Cuevas and Alumbaugh, 2011).*

The new vertical EM exploration method has been developed over the past few years by PetroMarker. The method operates in the time domain and uses stationary Vertical Electric Dipole (VED) sources that transmit a transient electromagnetic signal. Electromagnetic signal. When the source is turned on, a DC field diffuses outward both into the seawater

and into the subsurface. After a while, the source is turned off, inducing a secondary electromagnetic field that diffuses from the subsurface and back to the receivers, which record the vertical electric field component. The receivers are located at an offset range suitable for the method, typically 500–1,500 m. (as opposed to CSEM methods, which transmit and record simultaneously). A time-domain CSEM technique by *Barsukov et al. (2007)* also relies on injection of the electric current into the water using a vertical electric dipole. The vertical component Ez of the electric field is measured at the seabed after turning off the source current (Figure 6). This approach has a few positive features:
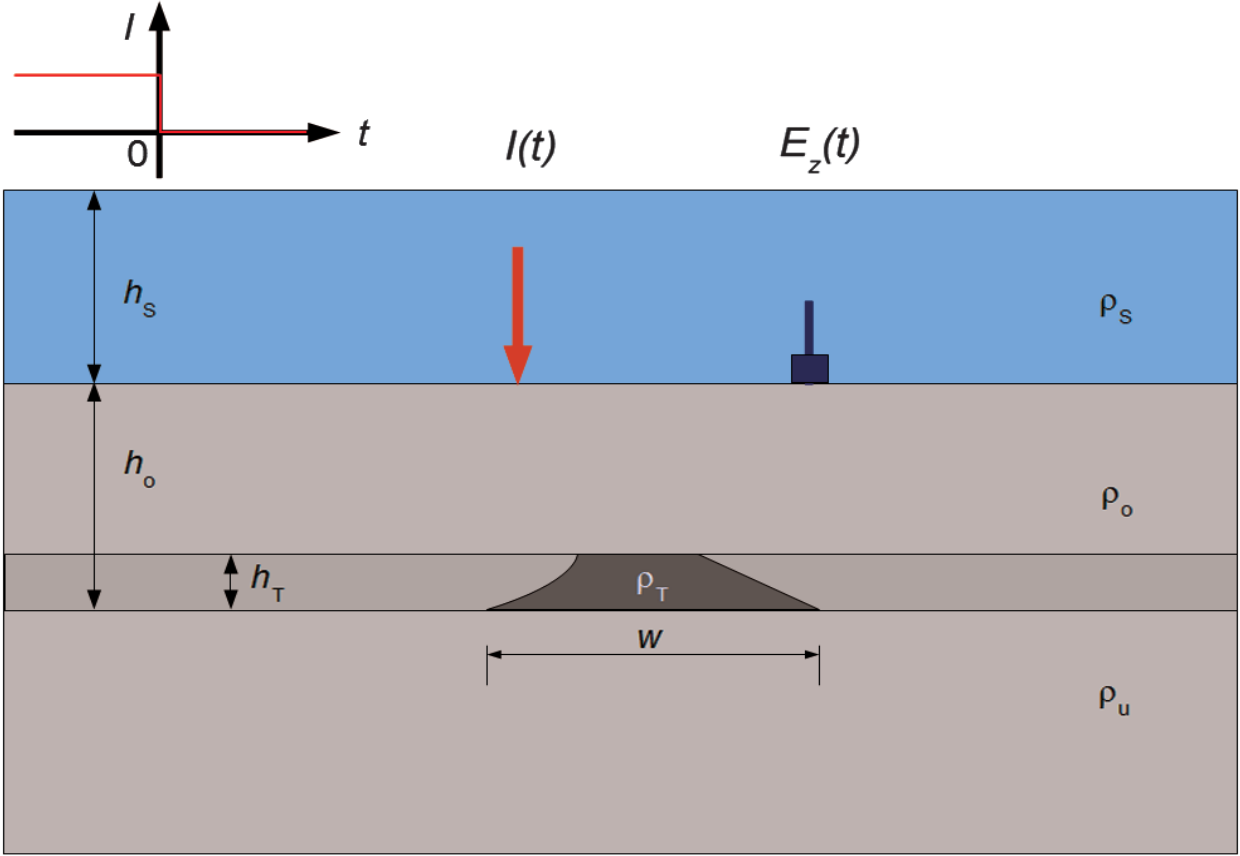
Figure 6. Schematic presentation of the acquisition system based on current injection using a vertical bipole and registration of the vertical component of the electric field. The injected current is switched off at t ¼ 0. Parameters hS, ho, hT indicate the water depth, the overburden, and reservoir thicknesses; ρS, ρo, ρu, ρT are the water, overburden, underburden, and reservoir resistivities; w specifies the horizontal extent of the reservoir. The case of w ¼ 0 corresponds to a stratified structure without a reservoir; the case of w ¼ ∞ corresponds to a stratified structure with the reservoir unlimited in both horizontal directions

A VED source does not create the TE-mode in a stratified medium, so that equations governs to

$$j = \sigma_b E = -\nabla_\tau \partial_z W + e_z \nabla_z^2 W$$

$$H = e_z \times \nabla_\tau W$$

The field is sensitive to relatively resistive layers. Compared to the traditional SBL approach, the measured signal is weaker, but it is usually preferable to directly measure small signals associated with the surveyed target, rather than to extract corresponding data from stronger signals contaminated by an unrelated to the target information. In particular, the VED source does not create an air-wave that dominates the SBL responses at large offsets *(Bension Sh. Et. Al., 2013).*

The vertical electric field is sensitive to deep resistive layers at late times the vertical electric field decays like $E_z(t) \approx t^{-5/2}$ over a rock of uniform conductivity. Using a vertical dipole and vertical receiver for marine borehole measurements has been suggested by *Scholl and Edwards (2007).*

Vertical transmitter (Figure 7.), is sensitive to horizontal resistive layers, and therefore carries information about the deeper structures. The upper electrode is kept at a fixed distance of 30-50m below sea surface independent of depth, to keep track of its position, and to utilize the maximum possible transmitter dipole length *(Terje Holten et. al. 2009).*

The magnitude of the external electromagnetic noise decreases with depth, because of the skin depth effect that dampens high frequencies. Hence, the signal-to-noise ratio usually increases with water depth. The advantage with time-domain measurements, is that there is no need for separation of the low amplitude signal from the deep layers from the noise resulting from the movement of the upper electrode. There is no air-wave because of the vertical transmitter, and the reduced signal level is the limiting factor for shallow water surveys.

The challenge when measuring the vertical, rather than the horizontal field, is the small amplitude of the signal. At late times the horizontal response from a horizontal dipole is 2−3 orders of magnitude stronger than the vertical response from a vertical dipole *(Chave and Cox, 1982).*

The optimal offset can be found, which is usually in the range from 500 m −1500 m. The response from the underground is recorded while the transmitter is off, so that the uncertainties of the location of the pulse electrodes do not lead to a time dependent noise. Verticality eliminates the air-wave components from the received signal.
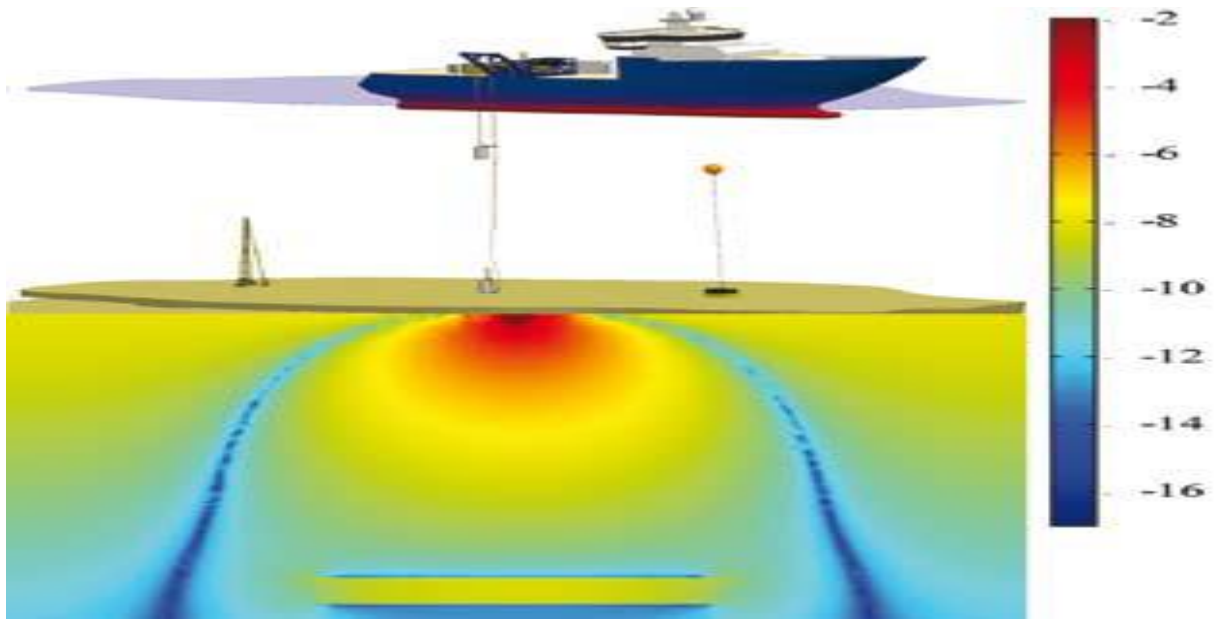
Figure 7. An overview of the Petromarker technology (not to scale), only one pulse system is shown. The upper and lower pulse electrodes which are directly on top of each other form the vertical transmitter dipole, the return current goes through the sea. To the left on the sea bottom, the extensible tripod is shown, and to the right, a flexible cable receiver. The colour scale (unit log10 (|Ez| (in V/m)) of the sediments represents the vertical electric field in the presence of the HC-filled reservoir (yellow). The electric field is evaluated for a 5000 Am source dipole shortly before the current is turned off.

1.4.5.1.3   Towed source EM (TSEM)

The current generation of the towed-streamer EM system consists of an electric Dipole source towed at a depth of 10 m below the sea surface, and up to a 9-km-long streamer of the electric field receivers towed at a depth of approximately 100 m. Figure 8 presents the corresponding layout of the towed-streamer EM system *(Anderson, C., and J. Mattsson, 2010).* The injected electric current from the source is transmitted as optimized repeated sequences (ORS), in which each sequence consists of a 100-s-long active part (source on) followed by a 20 s silent period (source off). The source sequence is designed to obtain as high energy as possible in a discrete set of frequencies, in which the electric field response is sensitive to the resistive anomaly. *Mattsson et al. (2012)* describe the deconvolution and current noise reduction methodology for the towed-streamer EM system.
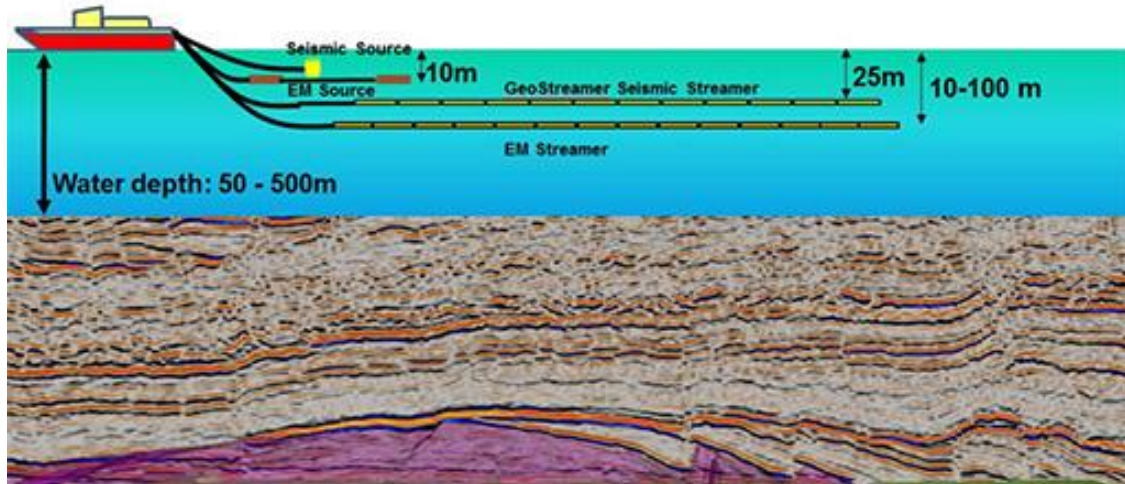
Figure 8. A sketch of the towed-streamer EM system.

The towed-streamer EM system makes it possible to collect EM data with a high production rate and over very large survey areas. At the same time, 3D inversion of the towed-streamer EM data is a very challenging problem because of the huge number of transmitter positions of the moving towed-streamer EM system, and, correspondingly, the huge number of the forward and inverse problems needed to be solved for every transmitter position over the large areas of the survey *(Ramananjaona, et. Al., 2011)*.

The prototype system described here is sufficiently powerful to work in water depths up to 400 m, with a nominal depth penetration of 2,000 m below the seafloor. The signal is a transient signal that can be a modified square-wave, or a PRBS *(Folke Engelmark, et. Al., 2012)*.

Towed EM, as described by *Anderson and Mattsson (2010)*, has numerous advantages:

- Improved efficiency: source and receiver towed from the same vessel.
- Operationally similar to marine seismic.
- Real time monitoring and QC of source and receiver cable.
- On-board pre-processing.
- Dense sub-surface sampling.
- Receivers towed above the seafloor. The influence of strong local anomalies at the seabed is minimized.
- Facilitates simultaneous acquisition of EM and 2D seismic.

The reason towed EM has not been available until now is that the relative movement between the receiver sensors and the seawater generate a voltage that is typically much

larger than the signal voltage. This was a crucial issue that had to be resolved before bringing the system to the market.

To characterize sensitivity of the CSEM method to the given target, we use the following quantity:

$$S = \frac{|E_{TA} - E_{BG}|}{\alpha|E_{BG}| + \eta}$$

The numerator represents the absolute value of the scattered field, i.e. the difference between the field in the presence of target E_{TA} and the background field E_{BG}, First, the sensitivity is computed as a function of the source receiver offset for a given frequency f and water depth*(D.V. Shantsev, F. Roth and H. Ramsfjell, 2012).*

The advantage of the deep towing is that very little EM energy is lost while propagating through the sea water, therefore it is preferred at larger water depths. We however demonstrate that in water depths of 250 m or less surface towing is likely to become the standard operation. At these depths, surface towing gives equally good results in terms of sensitivity and inversion as deep towing, while at the same time allowing a superior operational efficiency. The exact water depth threshold will depend on the specific target depth and geologic setting, and must be established through modeling and inversion during survey planning *(D.V. Shantsev, F. Roth and H. Ramsfjell, 2012).*

The relative uncertainty for a typical CSEM survey can be taken as 5% *(Zach et al., 2009)*.

The second term is the noise floor, which is determined by magneto-telluric noise, sensor noise, swell noise, etc. It is set to h = 10−15V/Am2 (after scaling by the source dipole moment).

First, the sensitivity is computed as a function of the source receiver offset for a given frequency f and water depth. Then we select its maximal value over all offsets and plot it as a map in the plane (f – water depth) in Figure 9.
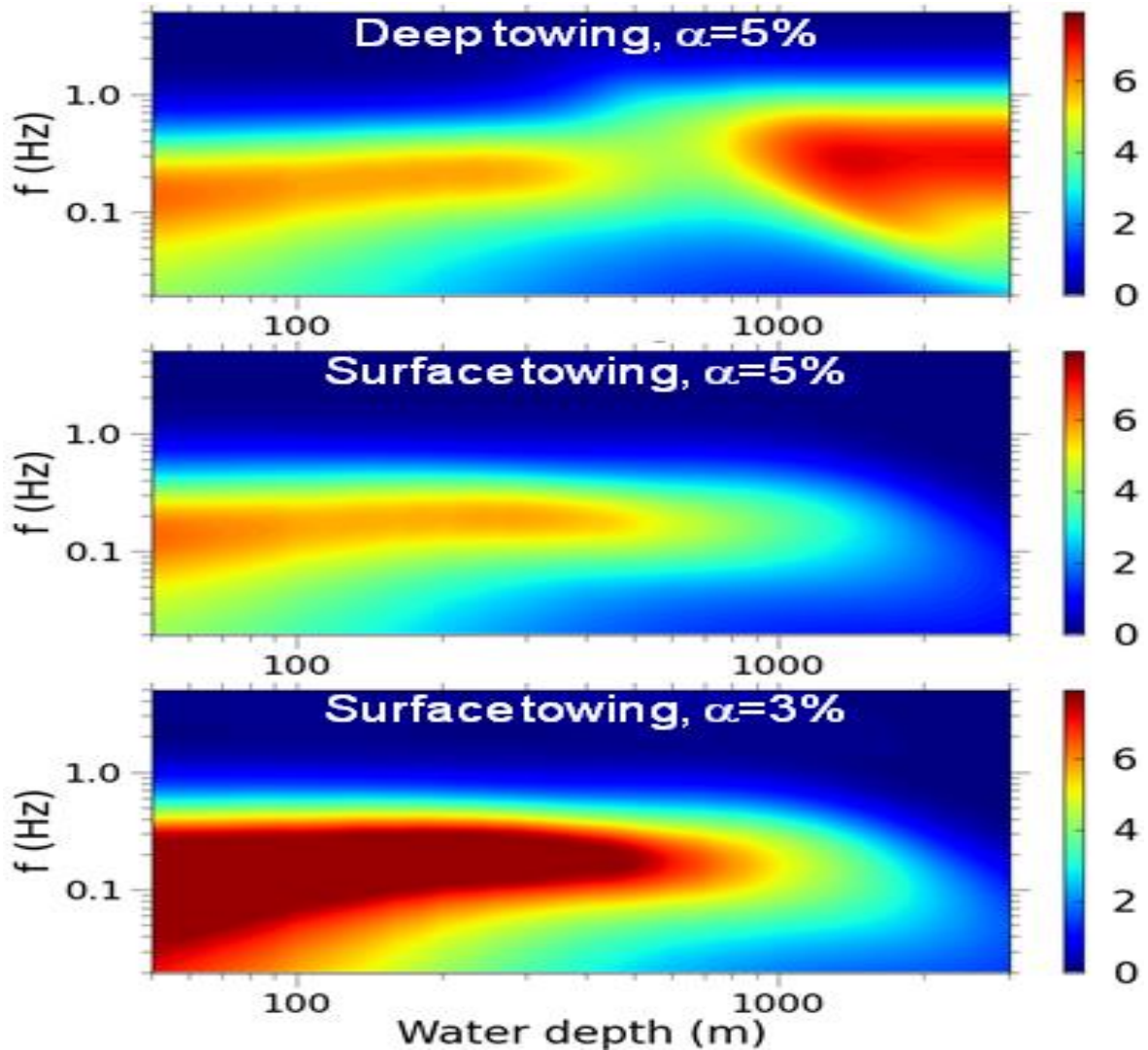
Figure 9. Sensitivity maps of the CSEM method for deep towing (top) and surface towing for a = 5% (middle) and a = 3% (bottom). The sensitivity is defined as the target response normalized to uncertainty, Eq. 1. The surface towing provides equal or better sensitivity if the water depth is smaller than 450 m. Reduction in the navigation uncertainty (a = 3%) moves the threshold depth to 700 m. Target depth is 2 km.

Obviating the need for ocean bottom receivers, the towed EM system enables CSEM data to be acquired simultaneously with seismic over very large areas in frontier and mature basins for higher production rates and relatively lower cost than conventional CSEM methods. The increased volume of CSEM data represents a challenge to existing 3D CSEM inversion methods.

1.4.5.2   CSEM Survey

Electromagnetic fields are useful in geophysics due to their interactive nature with the medium through which they propagate *(Zhdanov 2009).* This interaction can be used to

determine certain physical properties of rocks, these being electrical conductivity σ, dielectric permittivity ε, and magnetic permeability μ. The electromagnetic methods are based on the study of the propagation of electric currents and/or electromagnetic fields in the Earth.

Electrical resistivity of the subsurface provides important information on the porosity and pore geometry of the geologic formations as well as the nature of the fluids that fill the pore spaces. Resistivity increases exponentially for hydrocarbon bearing rocks, resulting into a strong resistivity contrast between gas-saturated and brine-saturated geological media. Until of recent, the seismic method has been the dominant technique used for reservoir detection and monitoring. Due to its shortcomings, different electromagnetic methods have been developed to detect and monitor geological hydrocarbons. Electromagnetic (EM) methods have provided a more cost effective monitoring technique that, at a minimum, has reduced the frequency of seismic surveys. CSEM which exploits the conductivity contrasts in the subsurface sediments has become an important complementary tool for offshore petroleum exploration prior to drilling *(Eidesmo, S. Ellingsrud et al. 2002, Mehta.K, Nabighian.M et al. 2005, Bakr and Mannseth 2009)*. Marine CSEM survey has been used in; estimating the formation resistivity without using borehole logs *(Constable and Weiss 2006)*, CO_2 sequestration monitoring *(Kang, Seol et al. 2011)*, and 3D modeling and time-lapse of CO_2 *(Bhuyian, Landrø et al. 2012)*. It can effectively detect marine reservoirs with high saturation of up to 60- 80% *(Wang, Luo et al. 2008, Constable 2010)*. This technique has been used mainly in discriminating between the hydrocarbon and the water-filled rocks in addition to estimating the geometry of the hydrocarbon *(Bhuyian, Landrø et al. 2012).* Hydrocarbons have a low conductivity less than 0.01 S/m while the formation water has a high conductivity of up to 10 S/m. Hence, the EM signal is strongly influenced by the porefluid contents *(Bhuyian, Landrø et al. 2012).*

1.4.5.2.1   Forward Modeling

Modeling data plays an important role in the standardization of the background field and the reservoir dimensions that play an important role during time-lapse CSEM monitoring. Time lapse CSEM can normally be used as a reservoir monitoring tool to help in the reservoir management *(Bhuyian, Landrø et al. 2012).* Assuming that other changes in the reservoir properties remain unaffected by the changes in the pore-fluid content, monitoring the production of hydrocarbons will help to observe and track any changes in the subsurface distribution through detection of changes in conductivity. The developed methods were tested for monitoring of geolectrical data to model the changes in saturation as reservoir production took place.

1.4.5.2.2　Inverse Modeling

Inversion of marine CSEM data has been previously done using Bayesian algorithm (*Ray and Key 2012*). *Torres-Verdin and Habashy (1995)* performed a linear inversion of 2D electrical conductivity. Basing on these studies, 3D inversion modeling of CSEM data has been done. In solving the inverse problems, the mathematical difficulty is that the inverse operator may not exist or may not be continuous over a given domain. Electromagnetic inversion methods are widely used in the interpretation of geophysical electromagnetic data in mineral, hydrocarbon, and underground water exploration. The EM response of the petroleum reservoir is weak compared to the background EM field generated by an electric dipole transmitter in layered geoelectric structures *(Zhdanov 2009)* ; thus rendering inversion of CSEM data a problem.

Bhuyian, Landrø et al. (2012) and Shahin, Key et al. (2010) noted that time-lapse CSEM data is achieved by carrying out several repeated surveys over a depleting reservoir at different times with the major aim of detecting and estimating the changes in the pore filling fluid properties. The main aim of CSEM monitoring is to image fluid flow in a reservoir during production since the electrical properties do change with fluid saturation. The monitoring process unlike exploration, is easily carried out and normally inexpensive since; (1) the same equipment used in the exploration are also used during the monitoring; (2) knowledge about the reservoir location and conductivity is acquired prior to monitoring; (3) the receivers being anchored on the seafloor reduces the experimental errors which would otherwise affect the process after subsequent surveys and ensures maximum mapping of the same target. According to *Lien and Mannseth (2008),* monitoring helps in determining the sensitivity of the CSEM data with respect to changes in conductivity distributions.

For enhanced oil production, brine or gas is injected into the depleted reservoir to displace the remaining oil towards the production well. Here, the main focus will be the detection of the electrical conductivity changes for a horizontal flooding with a two-phase zone separating the saline water and the saturated sediments; thus the reservoir being heterogeneous with varying brine saturations. As more conductive brine is injected into a depleted reservoir, conductivity increases there by decreasing the contrast. A decrease in conductivity contrast of the reservoir decreases the electric field indicating the change in the saturation of the hydrocarbon. Therefore, it will be expected that as more brine is injected, the formation resistivity of the reservoir increases. The extent to which the brine has migrated into the reservoir will be detected by the change in the anomalous electric field.

Inversion or "inverse modeling" attempts to reconstruct subsurface features from a given set of geophysical measurements, and to do so in a manner that the model response fits the observations *(Treite, et al., 1999).*
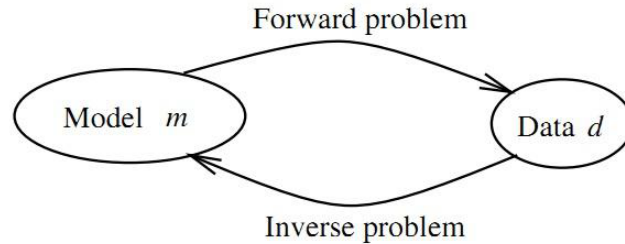

Figure 10. *Schematic representation of inverse modeling (Snieder, et al., 1999)*

1.4.5.3 Noise of System

The noise on the transmitter/receiver system represents an evident role in survey design. The CSEM noise is categorized as systematic and non-systematic noise. The first includes instruments noise and positioning error, further, its value is normally assumed to be proportional to the amplitude of the CSEM signal. The latter instead is independent of the signal, *Kwon (2003)* indicates a noise value of electric field equal to 0.5 V/m. The systematic noise decreases with the frequency since the amplitude of the signal tend to decreases increasing the frequency. We deduce that, for the lowest CSEM frequencies, from 0.1 to 2Hz, the systematic noise is predominant. *Constable and Weiss (2006)* has also derived the typical noise floor value due to the systematic noise component. For a receiver voltage noise Vr measured in V/m, a bandwidth B, and a source dipole moment SDM measured in A · m the electric-field noise is given by

$$E_n = \frac{V_r}{e(SDM)\sqrt{B}}$$

As example, for instruments having a voltage noise of 10−9V √Hz at 1 Hz and a source dipole moment of 450 KAm we get an electric-field noise of 2 · 10−15 V/Am2. Such value is assumed as the reference noise floor for CSEM systems. Data for interpretation are normalized by the dipole moment, so the system noise floor gets lower as SDM gets larger, allowing larger source-receiver offsets to be recorded and deeper structure to be detected. About the magnetic field, in literature *(Constable, 2010)* is indicated the reference value 10−18 1/m3 as noise floor (magnetic field normalized to the SDM).

1.4.5.3.1   Air Wave Effect

Of particular concern to companies who explore in shallow waters such as the shelf seas is the so called air wave. Some portion of the electromagnetic energy travels upwards to the sea surface, through the air to the vicinity of the receiver and then downwards to the receiver on the sea floor. The up over- down path can in some instances be faster than any direct path through the sea water or the subjacent crust. Compare the two models shown in Figure 11a, b and the stacked impulse response of these models shown in Figure 11c–f, for the in-line and broadside geometries. The sea layer in the first model is infinitely thick while that in the second has a finite thickness of 200 m. As the transmitter–receiver separation increases, the air wave which initially appears at later time appears to move to relatively earlier times and at large separations contaminates the disturbance travelling through the crust. From a practical point of view, the air wave signature is easily removed in the inversion of data provided sufficient dynamic range in the receiver electronics is available to record it properly *(Edwards, 2005)*.

(a) Double halfspace model with infinite sea layer

air layer

sea layer: σ_0=3 S/m

d_0: ∞

Tx   Rx

crust: σ_1=0.1 S/m

(b) Double halfspace model with thin sea layer

air layer: $\sigma = \infty$

sea layer: σ_0=3 S/m

d_0: 200m

Tx   Rx

crust: σ_1=0.1 S/m

(c) Inline Geometry

(d)

(e) Broadside Geometry
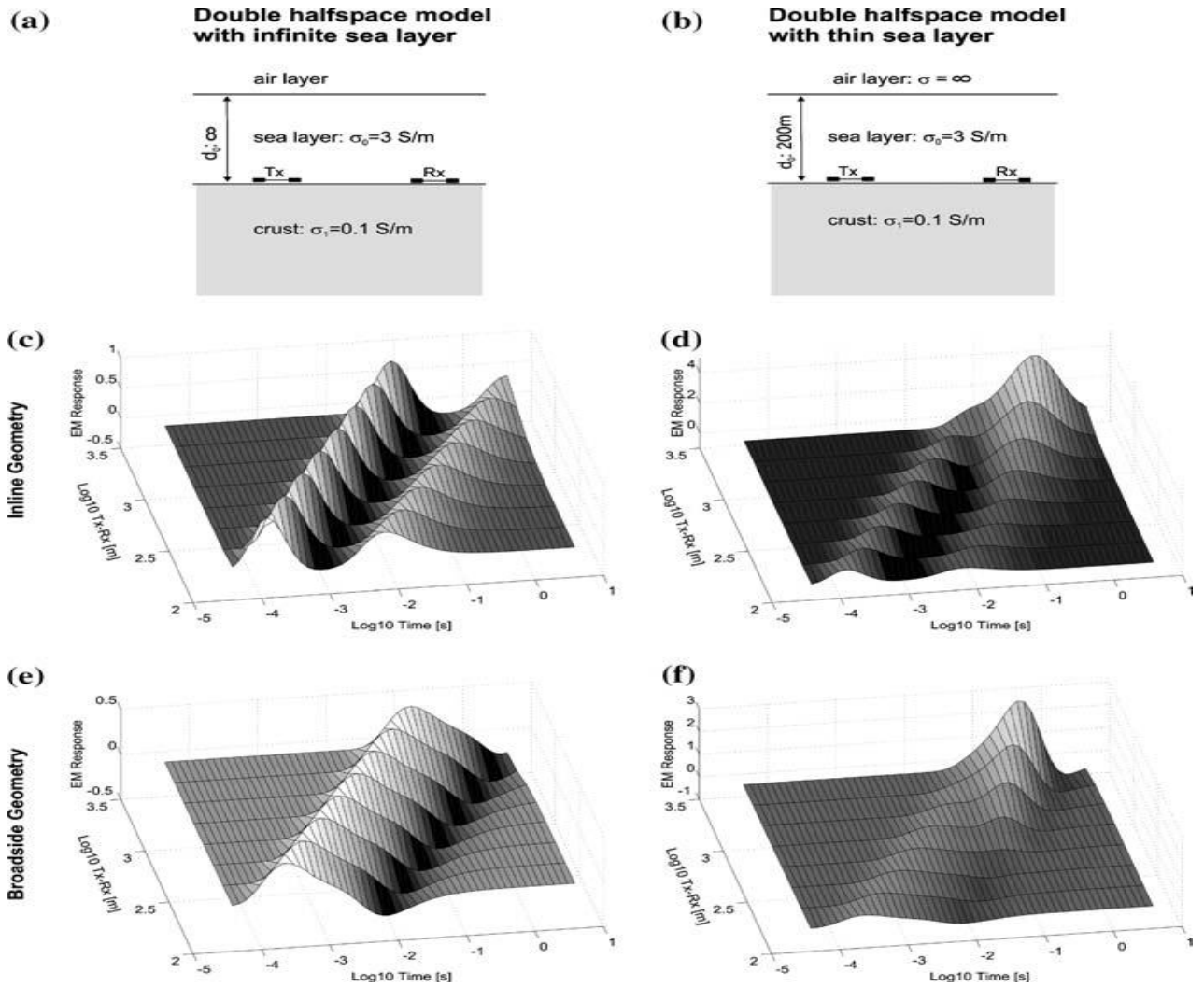
(f)

Figure 11. The airwave. The normalized impulse responses of the models in (a) and (b) to an electric dipole–dipole system on the seafloor are shown as functions of logarithmic time and transmitter receiver separation. Panels (c) and (d) refer to inline and panels (e) and (f) to broadside geometries.

29

Chapter 2   Applicability of 1D mCSEM modelling for HC exploration

I present one dimensional (1D) integral equation forward modelling of the marine controlled-source electromagnetic method. I apply the method to a synthetic model in the marine controlled-source electromagnetic exploration situation where conductivity is different from the known background medium.

I compare the results from 1D modelling, in all acquisition configurations , vertical, horizontal and shallow horizontal for a symmetrically placed reservoir, as a function of different frequencies in the cross-line direction, thickness, and for and depths. Depending on the model's parameters 1D modelling can be considered as an accurate and fast method for marine controlled-source electromagnetic acquisition optimization and interpretation.

The calculations have been done for two type of models (with target or without) which considering the sensitivity of parameters on each.

2.1 Theory

I investigate when a reservoir can be modeled as a volume of finite thickness (1D model), in this models we use the acquisition configuration for the sources and receivers which is shown in Figure 12.

In this model a single line of data is acquired with an in-line horizontal or vertical electric dipole source in the ocean and the resulting in-line electric field is measured by receivers located on the ocean bottom.

The background model consists of three layers; the upper space is air, the sea is modelled as a layer of finite thickness, and ground is modeled as a homogeneous space. A high-resistivity volume is located in the lower space. The models for 1D scattering objects are well-described in the literature, for example *Constable and Weiss (2006).*

The basic concept behind the method can be shown theoretically through examining the governing differential equations obtained from Maxwell's equations. Which is presented in following section (1.4.5.1.2 and 1.4.3).
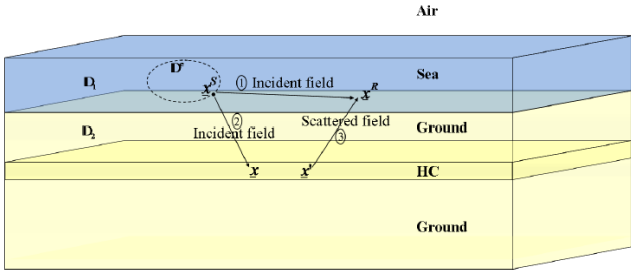

Figure 12. Schematic diagram of Diffusive fields present in a three horizontally stratified earth layer configuration for both forward source and scattering problems.

2.2 Forward Modeling

The forward model is the link between the model and data parameters according to the nonlinear relation:

$$d = g (m)$$

It is used to predict, for a given set of model parameters m ∈ M, the values of the observable parameters d ∈ D. In this study, the non-linear vectorial function g is a numeric electromagnetic simulator, since in the study of electromagnetic fields, no solution-closed form exists, with the exception of few analytical cases. The electromagnetic simulator implements the Finite Element Method for 1D geometry. 1D geometry means that forward model assumes that electromagnetic properties (relative permittivity, relative permeability, electric conductivity, magnetic conductivity) do not vary along one axis, and all the sources lie on the same plane orthogonal to that axis. This assumption allows to reduce the dimensionality of the electromagnetic problem reducing resources and time consumption. Further details on the CSEM simulator are available in the reference *(Oldoni M. 2011).*

2.3 A 1D forward code

Based on the theory presented, I have used a Matlab program (OCCAM1D mCSEM) which has been developed by "Kerry key - Scripps Institution of Oceanography" that can calculate the 1D layered Earth response for a dipole-dipole CSEM arraying all vertical and horizontal position of dipoles. Such a code is needed for forward and inverse modeling of data. Previous software written for this purpose was developed by Nigel Edwards in FORTRAN; however, as Matlab is a far more common numerical software language, an update of this 1D forward code was needed. The software takes as input the resistivity, frequency rotational angle of dipoles, dipole length and thickness of a series of layers and calculates the recursion relations which is explained in Appendix A & B.

2.4 Modeling scenario and description

The data utilized for thesis simulation has been extracted from the 1D model simulated in MATLAB computing environment (OCCAM1D). The model has been inspired from the interpretation of marine CSEM data which have been obtained by EDISON Co. The Model presents the amplitude and phase curves versus source-receiver offset for canonical reservoir model with three configurations (see figures 13 - 15); a 100-Ωm reservoir 100-m thick, buried at a depth of 1700 m, 300 m of sea depth, in a host sediment of 10 Ωm in 1600-m depth. Additionally, the transmission frequencies of 0.2Hz, 0.48 Hz, 0.76 Hz, and 1.04 Hz have been used to highlight all the dominant propagation paths.
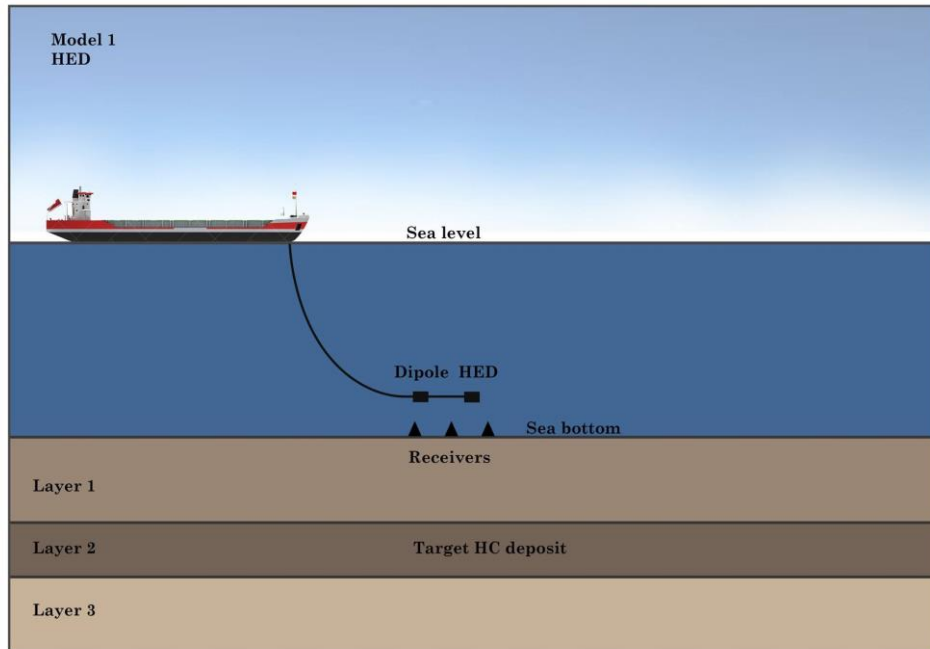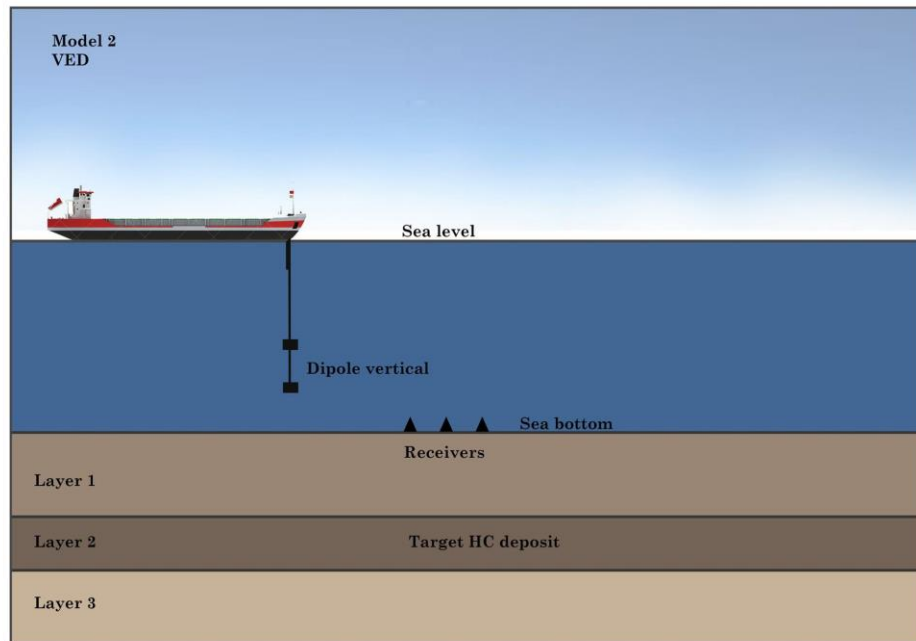
Figure 13. HED configuration
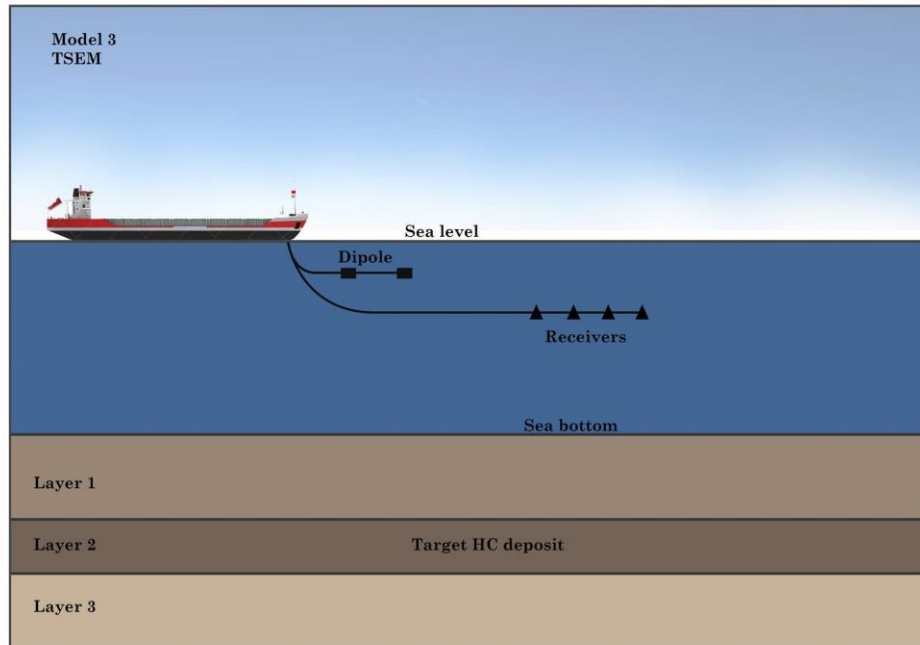

Figure 14. VED configuration

Figure 15. TSEM Configuration

2.4.1 Model Dataset

The data contains electric field components (amplitude and phase) observation from a hypothesized and simulated marine controlled source electromagnetic (mCSEM) survey. The acquisition geometry is assumed in line with 70 transmitters and receiver gathers having a spacing of 110 meters respectively.

Four marine CSEM frequencies were used for the data generation, i.e., 0.20 Hz, 0.48 Hz, 0.76 Hz and 1.04 Hz and transmission is assumed to be from a horizontal electric dipole (HED), vertical electric dipole (VED) and towed stream electromagnetic (TSEM). It contains information about the coordinates and locations x; z (in meters) of transmitters (Tx) and receivers (Rx) in the subfields.

The amplitude of the electric field (Ex, Ez) for each receiver is in linear scale and the simulated data contains both an anomalous part of the amplitude component of the electric field and that without anomaly which is referred to as background. The data is totally devoid of noise and the amplitude of the electric fields are in units of V/Am^2 while the phase are in degrees.

2.4.2 Model description

The inspired 1D model consists of two different parts; namely fixed and varying parts. The fixed part of the model is made up of fixed parameters' values consisting of an upper air layer of relative dielectric constant εr = 1 and zero conductivity (σ = 0 S/m), the water layer of 300 m meters (εr = 80 and σ = 3 S/m), and a uniform below sea background medium (εr = 1, σ = 1 S/m). The varying part of the model consists of an anomalous layer embedded in the background medium which has been shown in figure 13 (whit and without HC) according the resistivity, with varying thickness, depth below the sea bottom and conductivity. Also the simulated acquisitions are performed at different frequencies. It should be indicated that in the further calculations and data analysis, resistivity factor (ρ) has been implemented instead of the conductivity factor (σ), where $\rho = \frac{1}{\sigma}$.
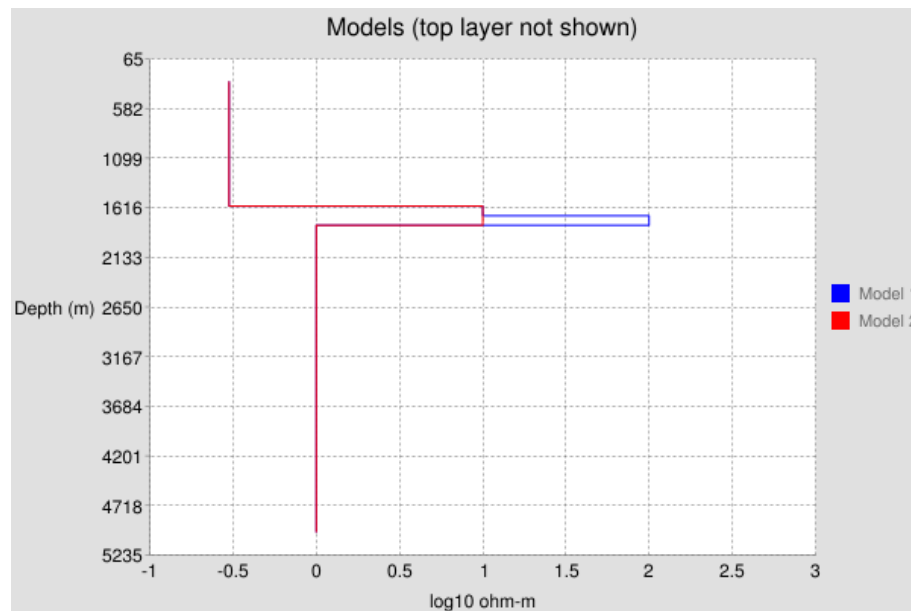

Figure 16. Resistivity Model

The varying part of the models (with and without target) consists of an anomalous layer embedded in the background medium, with varying depth below the sea bottom and conductivity. Also the simulated acquisitions are performed at different frequencies. The range of the variable parameters are reported in Table 1 and 2.

MODEL 1	Unit	Range
Frequency	Hz	0.2 – 1.04
Thickness	m	100
Resistivity	Ohm-m	100
Depth	m	1700

MODEL 2	Unit	Range
Frequency	Hz	0.2 – 1.04
Thickness	m	100
Resistivity	Ohm-m	-
Depth	m	1700

Table 2. Model without hydrocarbon deposit in depth (Homogenous medium)

Moreover, the model is built considering 70 receivers (Rx) with height of one meter over the sea bottom and electric field source (transmitter Tx) towed 30 meters above the sea bottom and use for three types of acquisition methods (VED, HED and TSEM). The maximum offset (distance between transmitter and receiver) is 7700 meters (Figures 13-15).

2.4.3 Model output

The simulation code (OCCAM1D – Dipole_1D) derives the amplitude and phase of electric and magnetic fields with respect to offset at each receiver station which are called magnitude versus offset (MVO) and phase versus offset (PVO). Sample MVO and PVO plots from vertical, horizontal antenna are shown in the Figures 18 – 25, for both the background without resistive anomaly and the data with anomaly. The outcome of this processing is the superimposed mapping of the extracted magnitude/amplitude component of the electric field responses of the background and anomalous data for different acquisition frequencies.

2.4.3.1   Result of HED Acquisition

Solid line: Model 1, Dashed Line: Model 2

In this case the receivers laid down at depth of 300m and transmitters installed at depth of 270m.
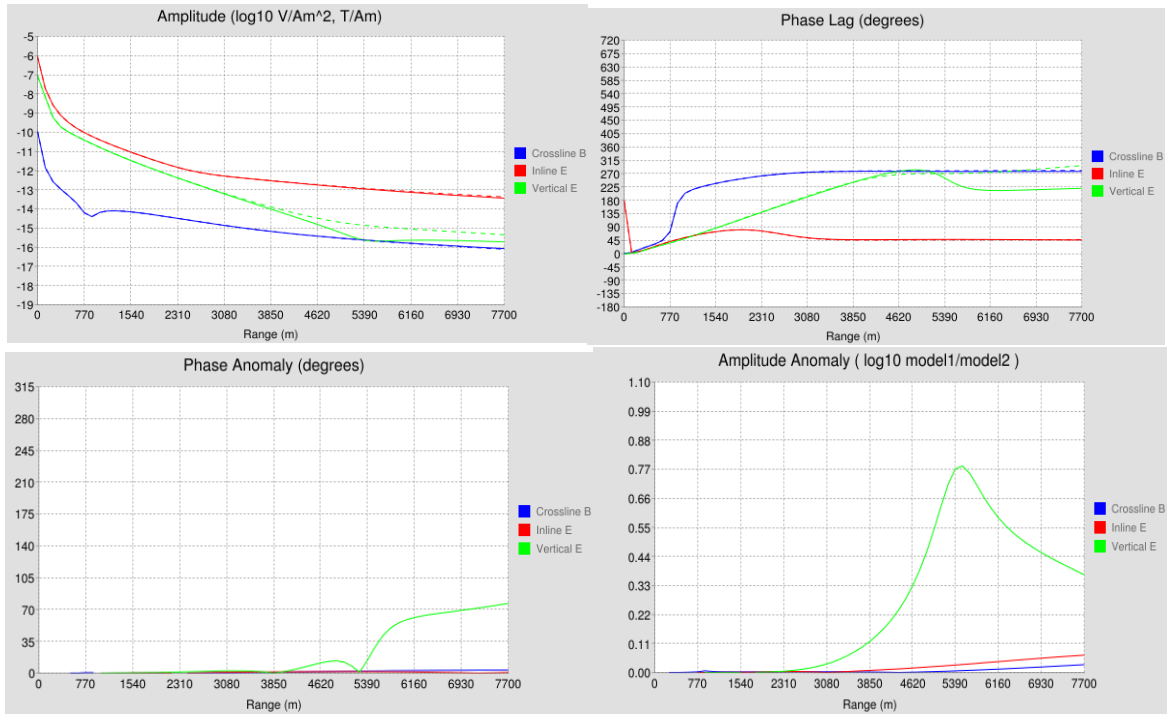
Figure 17 Magnitude versus offset (MVO) and Phase versus offset (PVO) with frequency of 0.20Hz
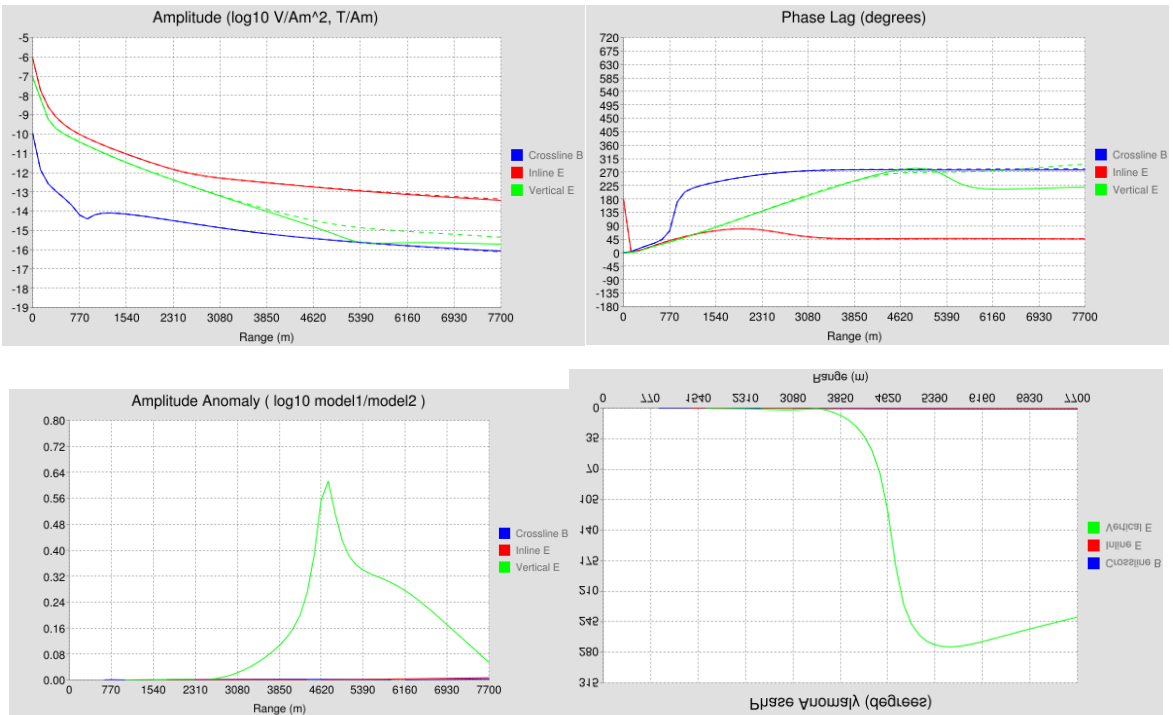

Figure 18. Magnitude versus offset (MVO) and Phase versus offset (PVO) with frequency of 0.48Hz

Figure 19. Magnitude versus offset (MVO) and Phase versus offset (PVO) with frequency of 0.76Hz

Figure 20. Magnitude versus offset (MVO) and Phase versus offset (PVO) with frequency of 1.04Hz

2.4.3.2   Result of VED Acquisition

Solid line: Model 1, Dashed Line: Model 2

In this case the receivers laid down at depth of 300m and transmitters installed at depth of 270m.

Figure 21. Magnitude versus offset (MVO) and Phase versus offset (PVO) with frequency of 0.20Hz

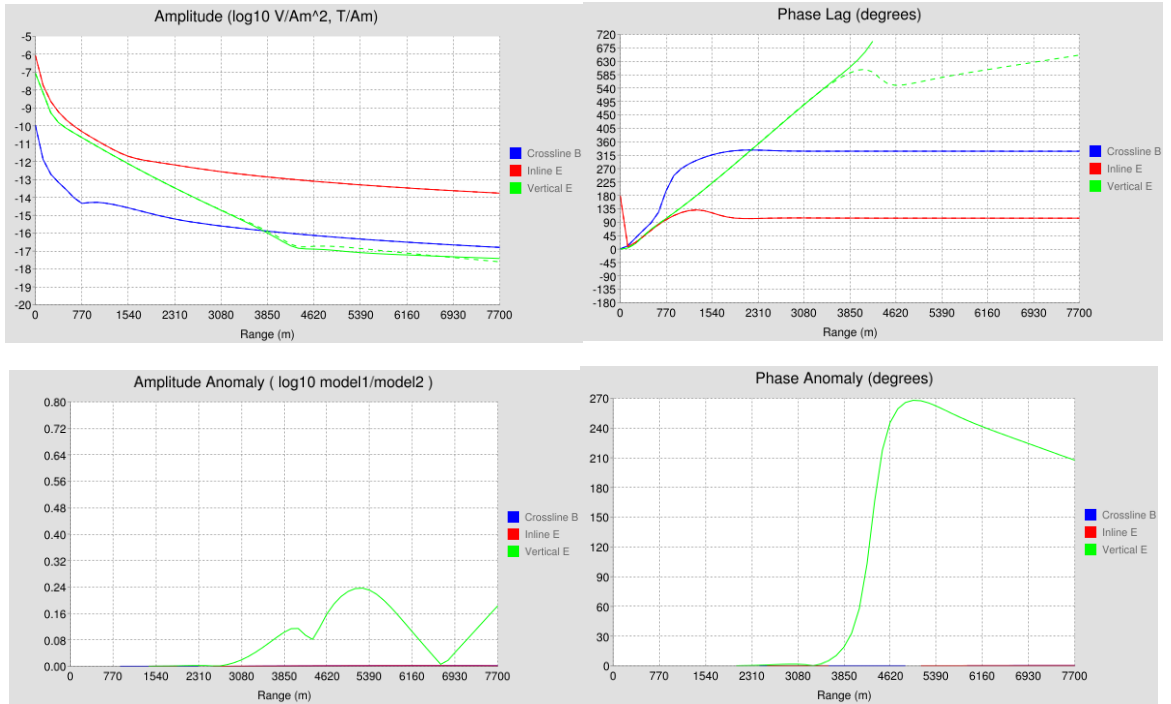*Figure 22. Magnitude versus offset (MVO) and Phase versus offset (PVO) with frequency of 0.48Hz*

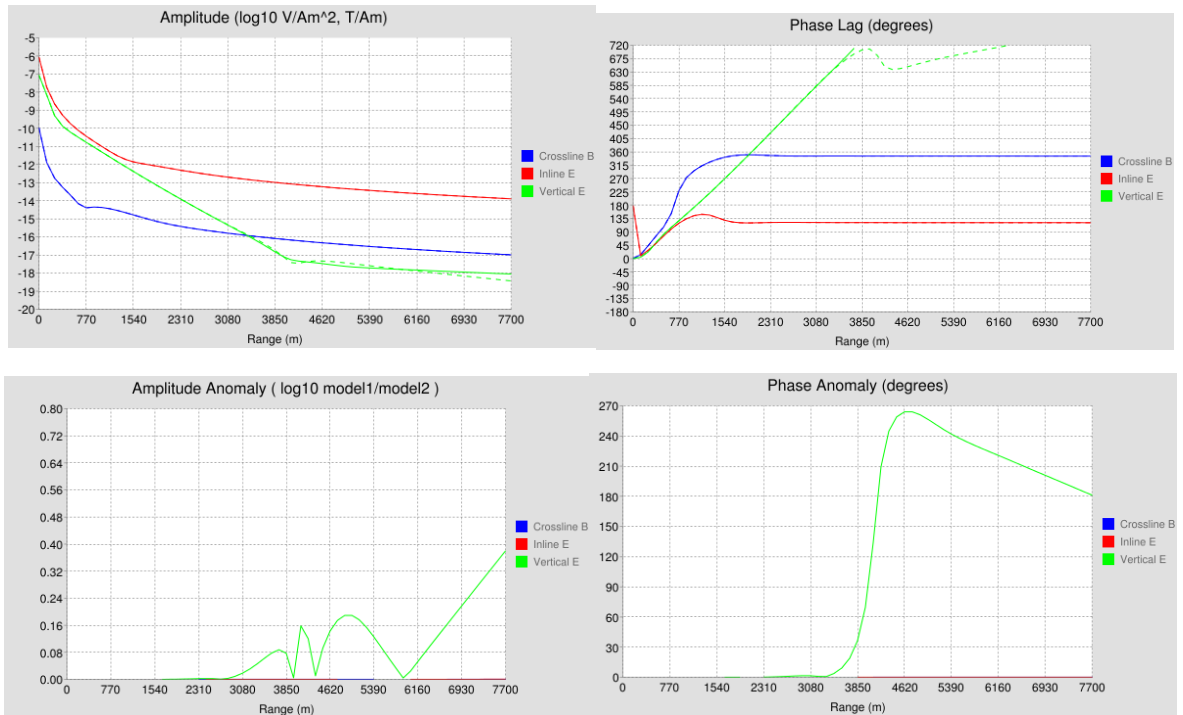*Figure 23. Magnitude versus offset (MVO) and Phase versus offset (PVO) with frequency of 0.76Hz*

Figure 24. Magnitude versus offset (MVO) and Phase versus offset (PVO) with frequency of 1.04Hz

2.4.3.3   Result of TSEM Acquisition

Solid line: Model 1, Dashed Line: Model 2

Transmitter depth in this method has been located at 10m below sea level but the receivers located at 100m below.
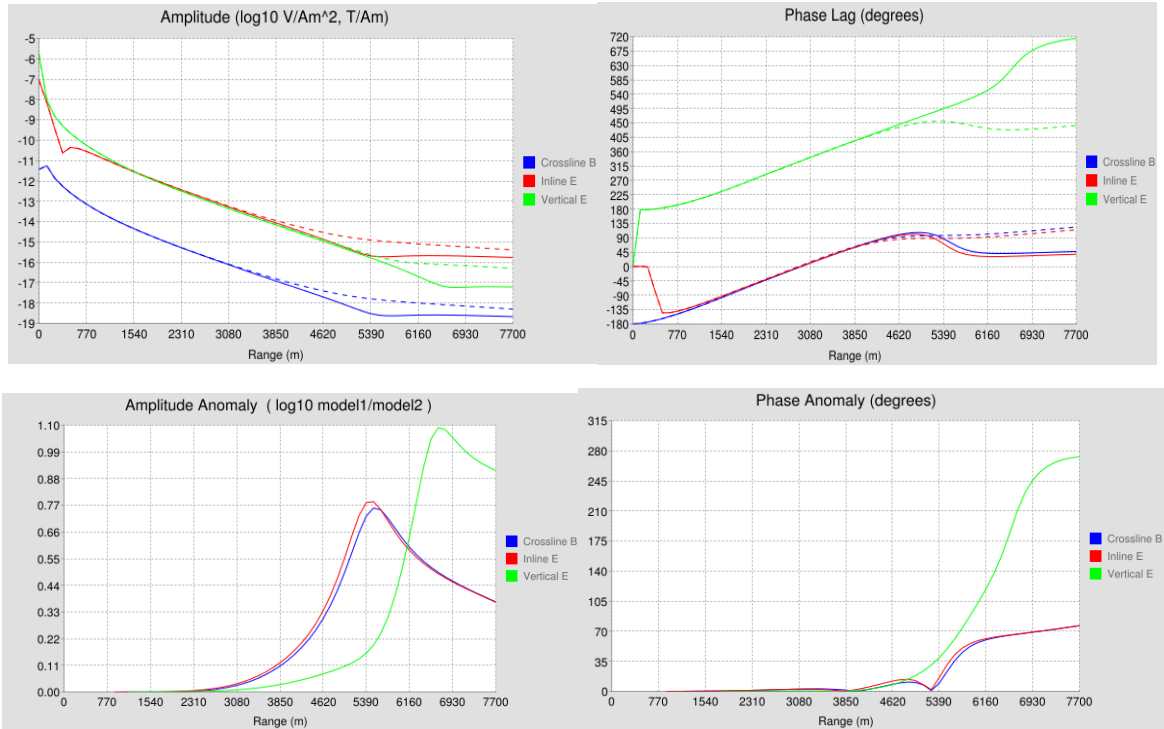

Figure 25. Magnitude versus offset (MVO) and Phase versus offset (PVO) with frequency of 0.20Hz

Figure 26. Magnitude versus offset (MVO) and Phase versus offset (PVO) with frequency of 0.48Hz
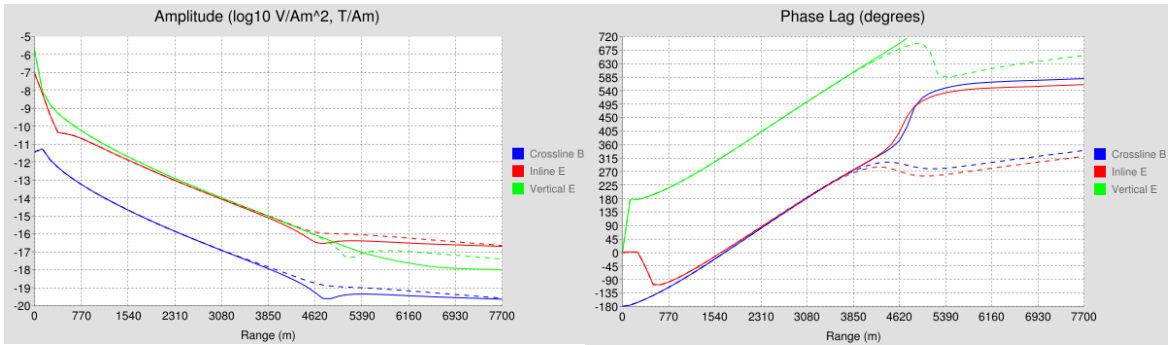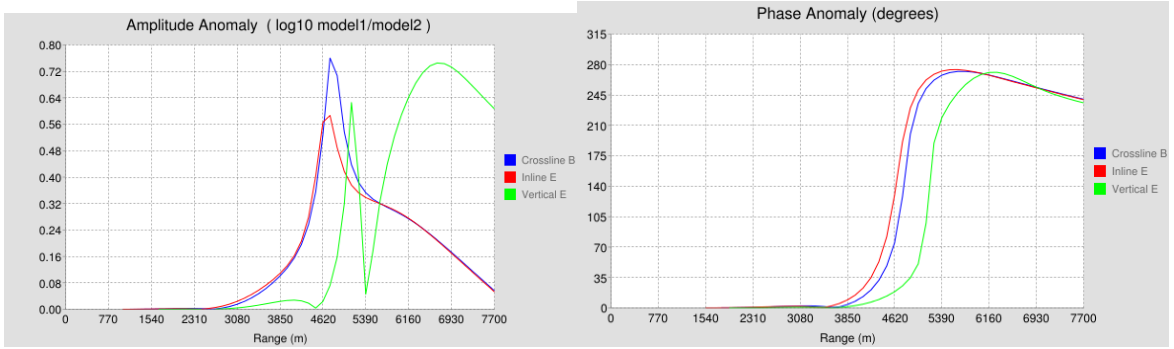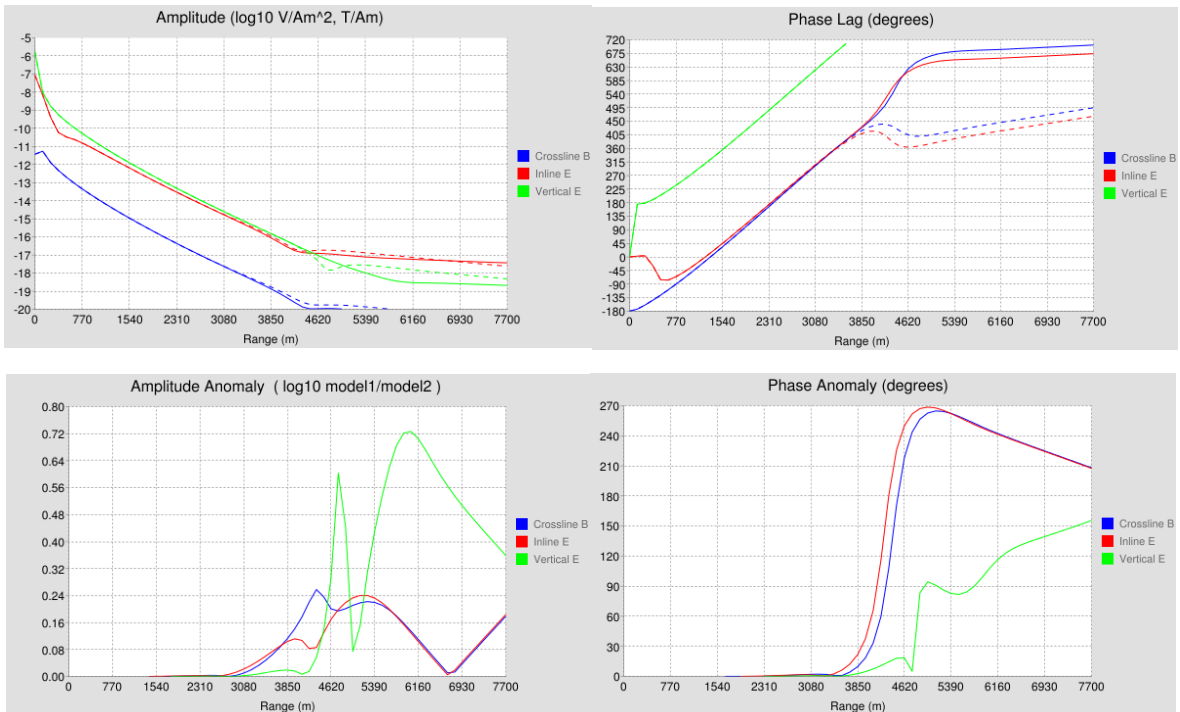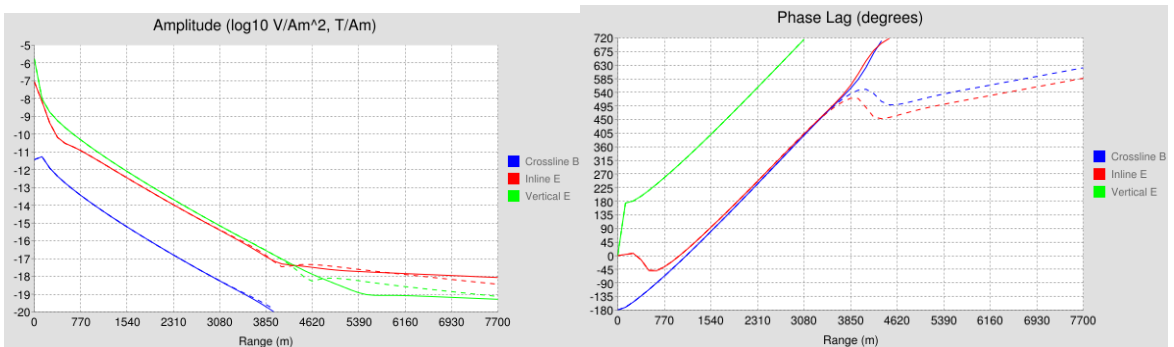
41

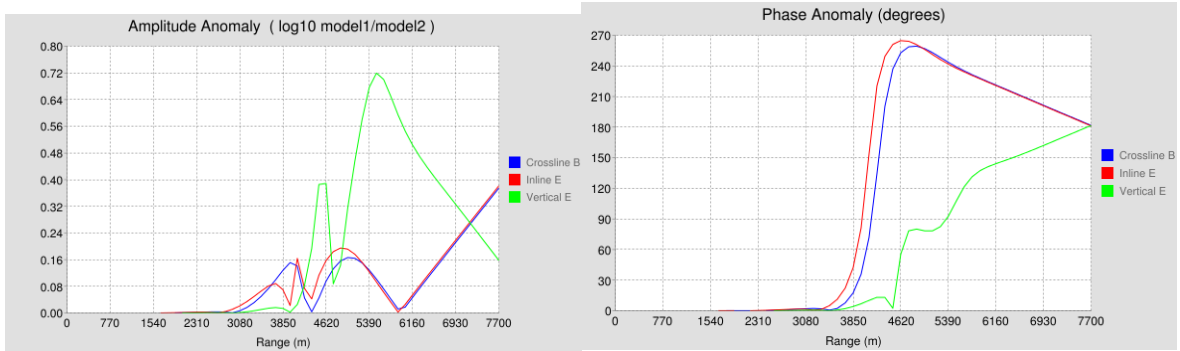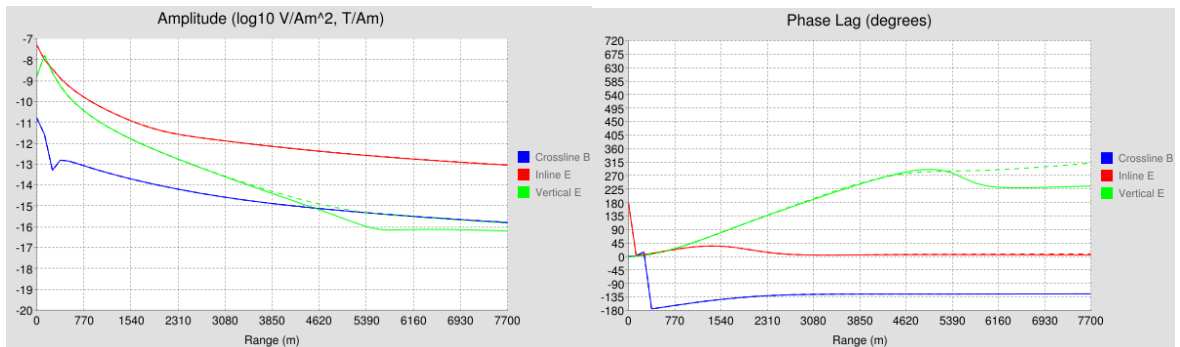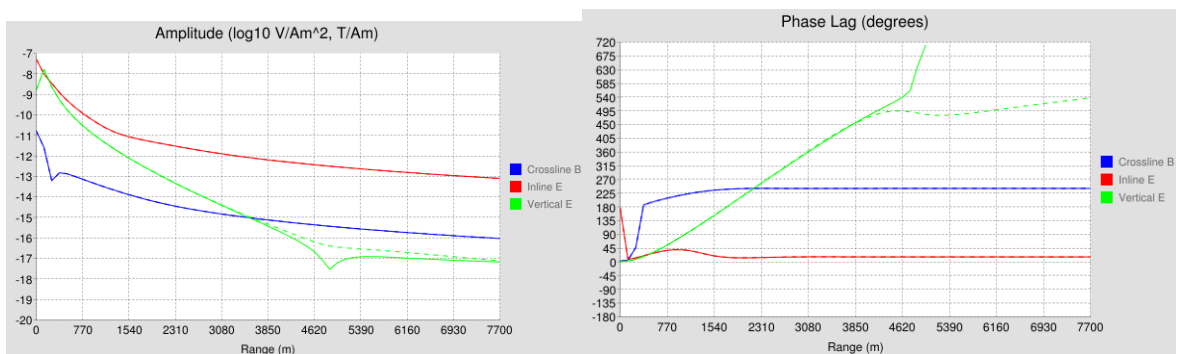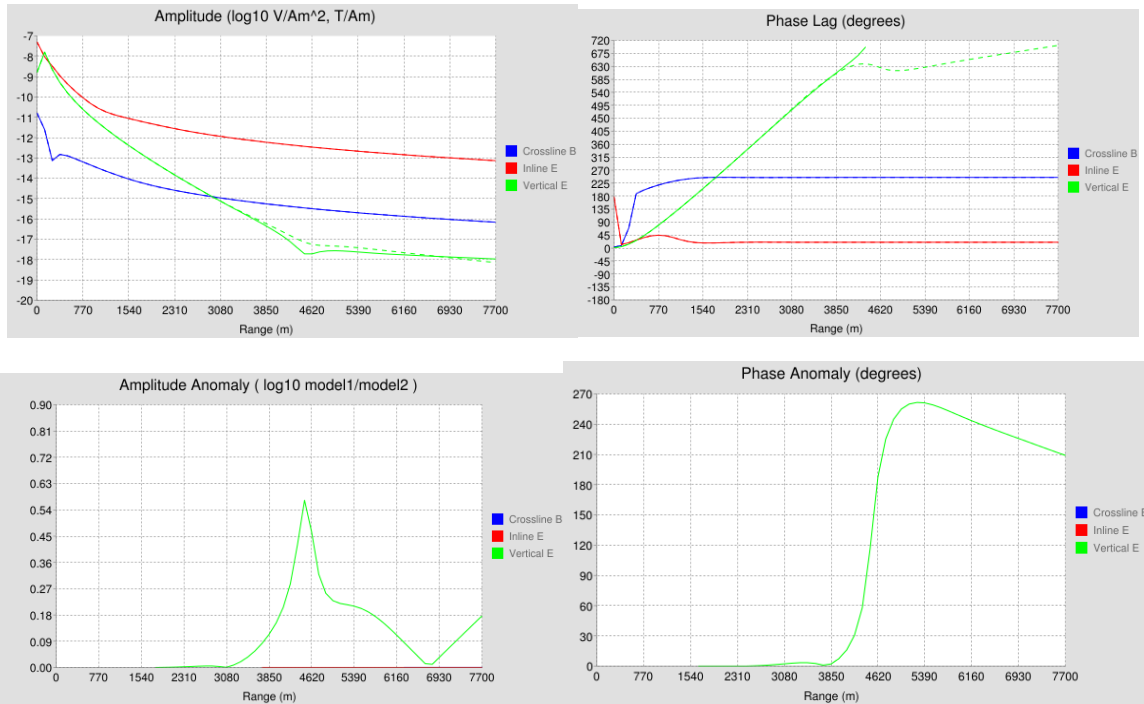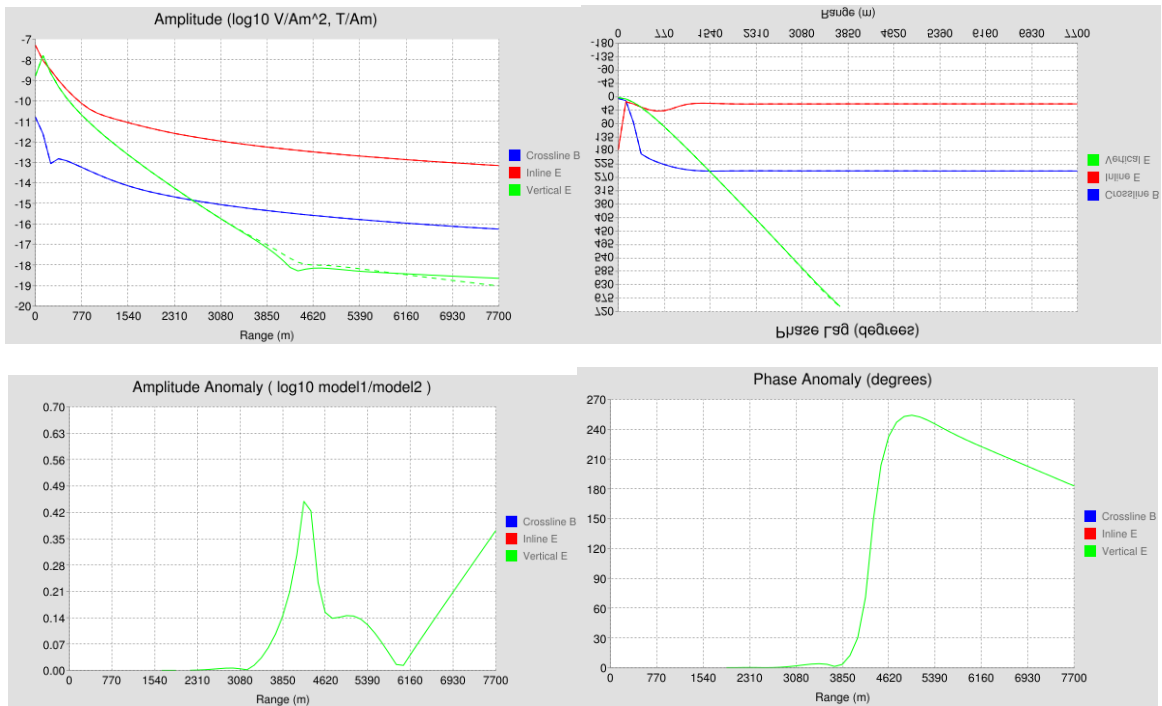*Figure 27. Magnitude versus offset (MVO) and Phase versus offset (PVO) with frequency of 0.76Hz*

Figure 28. Magnitude versus offset (MVO) and Phase versus offset (PVO) with frequency of 1.04Hz

42

It should be mentioned that for sake of simplicity, the Ez (electric field amplitude in Z direction) has been calculated in vertical antenna. As additional information, the vertical measurement (Ez) is useful for discriminating deep resistive targets even at very close source receiver offsets *(Alumbaugh, et al., 2010).*

To understand how the result of Model (with target) changing by different thicknesses to considering the sensitivity respond we applied two different thicknesses to the model for three type of configurations and reach the results which is seen in figure..

2.4.4 Inversion Problem

2.4.4.1   Objectives

Solving geophysical inverse problem for estimation of resistivity distribution in an investigated area is known to be ill-posed giving rise to a non-unique solution. Moreover, solving inverse problems is always likely to demand a high computational cost, thus utilizing preliminary information about the model to be estimated constrains the inverse problem making the solution better.

Complex mathematical approaches, such as adjoint and Green's functions *(Farquharson, 1995)*, have been used to produce numerical value for the sensitivity.

It also compares the results obtained using the sensitivity analysis at different offsets with respect the various frequencies for controlling the resistivity model which is approached by Inversion technique.

2.4.4.2   General Introduction

The scientific procedure for the study of a physical system can be (rather arbitrarily) divided into the following three steps.

i)   Parameterization of the system: discovery of a minimal set of model parameters whose values completely characterize the system (from a given point of view).

ii)   Forward modeling: discovery of the physical laws allowing us, for given values of the model parameters, to make predictions on the results of measurements on some observable parameters.

iii)   Inverse modeling: use of the actual results of some measurements of the observable parameters to infer the actual values of the model parameters.

Strong feedback exists between these steps, and a dramatic advance in one of them is usually followed by advances in the other two. While the first two steps are mainly inductive, the third step is deductive. This means that the rules of thinking that we follow in the first two steps are difficult to make explicit. On the contrary, the mathematical theory of logic (completed with probability theory) seems to apply quite well to the third step, to which this book is devoted. *(Albert Tarantola 2005)*

2.4.4.3   The CSEM inverse problem

Understand how the signals propagate in the model, explanation of the phenomena studying the signal propagation in a layered structure is the concept of inversion problem.

With reference to the Figure 12, the total electric field at the receiver can be generalized as, in first approximation, as the sum of the following five contributions:

• The lateral wave on the sea-surface interface, (negligible in deep water)

• The direct wave source-receiver,

• The lateral wave on the seabed interface,

• The reflected wave from the thin layer,

• The guided wave in the thin layer, (if the reservoir is more resistive than sub seafloor).

A more quantitative analysis of the field propagation can be performed by analyzing separately the previous field contribution, through the decomposition of the electromagnetic field in the transverse electric polarization (TE mode) and the transverse magnetic polarization (TM mode). Then, in first approximation, the total electromagnetic field collected by receivers, is obtained by applying the superposition principle.

2.4.4.4   Theory of inversion

The inversion procedure is based on the probabilistic approach introduced by *Tarantola (2005)*. In this way we are able to describe, through probability densities, model and data uncertainties, as well as any prior information we have on the particular scenario. As explained in the first part of the thesis, the solution of the inverse problem is obtained through an iterative procedure that linearizes the forward model around the current model m_k.

$$d - d_k = G(m - m_k)$$

At each iteration a new model m_{k+1} is obtained using the Jacobean matrix G_k of the derivatives of the forward model equation with respect to the current model parameters.

The model updating is given by:

$$\underline{m}_{k+1} = \underline{m}_{prior} - \left[\underline{G}_k^T \underline{C}_d^{-1} \underline{G}_k + \underline{C}_M^{-1}\right] \underline{G}_k^T \underline{C}_d^{-1} \left[g\left(\underline{m}_k - \underline{d}\right) - \underline{G}_k\left(\underline{m}_k - \underline{m}_{prior}\right)\right]$$

We define prior uncertainties with Gaussian probabilities. The state of information on the model parameters is described by the prior model m_{prior} and by CM, the covariance matrix that takes into account its uncertainties. We assume as prior model the background model, represented by a homogeneous medium having electric conductivity of 1 m. The cardinality

of the vector model is 20, corresponding to the number of macro regions Nm: m_{prior} = [ρ1, ρ2,.., ρn.., ρNm]T ρn = 1, n = 1, ...Nm (5.15)

The covariance matrix CM is a diagonal matrix defined as: CM = σ2·I_{20x20},

Figure 5.15. The standard deviation associated to each single model parameter is set to $30 Ohm - m$. This value is a compromise because it allows to reach higher resistivity values in few iterations without losing too much resolution in the model parameter estimation.

Cd is the covariance matrix that takes into account the uncertainties due to both the measurements and the modelling since under Gaussian uncertainties assumption we have Cd = CD +Cg. A common way to set the data covariance matrix consists of considering the precision of the receiver which has collected the measurements. In this synthetic example, we have built the data covariance matrix setting the standard deviation of the data components as follow:

-   Standard deviation of the magnitude (subscript m) of the normalized fields:
    σm,Ex = σm,Ez = σm,Hy = 0.05
-   Standard deviation of the unwrapped phase (subscript φ) of the normalized fields:
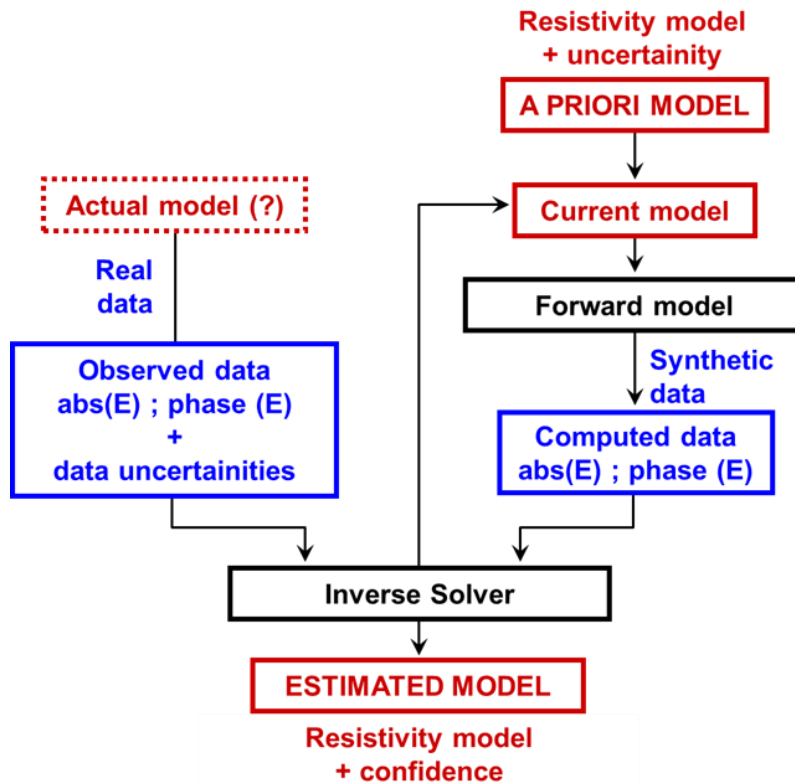   σ+,Ex = σ+,Ez = +,Hy = 0.05 rad ≈ 2.9。

Figure 29.Regularization with data and model reliability

2.4.4.5 Scenario for Inversion problem

The inspired 1D model of inversion is a promising approach for exploration in basalt covered areas which the data has been collected from Faroe Island Project. The fixed part of the model is made up of fixed parameters' values consisting of an upper air layer of relative dielectric constant $\varepsilon r = 1$ and zero conductivity ($\sigma = 0$ S/m), the water layer of 1000m to 700 meters ($\varepsilon r = 80$ and $\sigma = 3$ S/m), and a uniform below sea background medium ($\varepsilon r = 1$, $\sigma = 1$ S/m). The varying part of the model consists of an anomalous layer embedded in the background medium which has been shown in figure 30 (whit massive and thin layers of basalt) according the resistivity, with varying thickness, depth below the sea bottom and conductivity. Also the simulated acquisitions are performed at different frequencies.
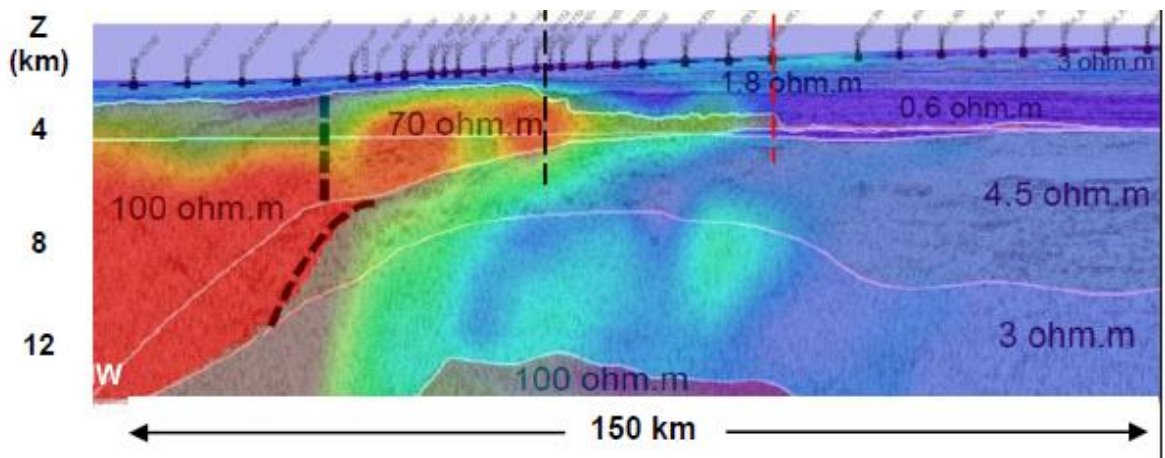
Figure 30. Resistivity model Profile of CSEM attribute for different frequencies.

As we can see the target area is divide into two part which involve the high resistivity and low one, in order to, the inversion calculation has been done in massive basalt area which is shown by vertical dash line in figure 30.

The models parameter and calculation are based on the resistivity and thickness which is inserted to the software that has been developed by Politecnico di Milano department of electronic and information, CSEM Group.(see figure 31.)

./save/faroer1 TX 0001 20160330 113558

A priori model

	rho [ohm.m]	I	thk [m]	I	zone [2:water, 3:solid]	type [1:layer, 2:gradie...	Add/remove
1	0.3000 ☐		2200 ☐		2	1	☐
2	1.1496 ☑		60.9381 ☑		3	1	☐
3	2.4839 ☑		1.0444e+03 ☑		3	1	☐
4	1.4072 ☑		238.2378 ☑		3	1	☐
5	186.1333 ☑		100 ☐		3	1	☐

- Prior model: Model.000

	rho [ohm.m]	I	thk [m]	I	zone [2:water, 3:solid]	type [1:layer, 2:gradie...	Add/remove
1	0.3000 ☐		2200 ☐		2	1	☐
2	1.1496 ☑		60.9381 ☑		3	1	☐
3	2.4839 ☑		1.0444e+03 ☑		3	1	☐
4	1.4072 ☑		238.2378 ☑		3	1	☐
5	186.1333 ☑		100 ☐		3	1	☐

```
30-Mar-2016 11:34:45 - Starting CSEM 1D Inverter
===> Loaded model file Faroer_final1.mat
-------------------------
===> 30-Mar-2016 11:35:18 - Inversion of TX 1
-> Data in file ./save/faroer1_TX_0001_20160330_113517
-------------------------
===> 30-Mar-2016 11:35:59 - Inversion of TX 1
-> Data in file ./save/faroer1_TX_0001_20160330_113558
```

Model params | Runtime Figures | Conditioning Analysis

MODEL PARS | INVERSION PARS | ADVANCED PARS

MODNAME (savefile prefix)	faroer1
Minimum offset [m]	1400
Maximum offset [m]	10000
Reference zero phase offset [m]	1400
Index of frequencies to invert	1 2 3 4 5 6
Index of TX gather to invert	1
Heigth of TX over sea bottom [m]	45
Heigth of RX over sea bottom [m]	1
Nr. of simulated RX (then interpolation)	12
Layer interpolation	cubic2

- Prior m... | Ready

Start inversion
Save & stop at end of iteration ○
Stop ASAP ○
Load XLS model | Save XLS model
Load MAT (model & pars) | Save MAT (model & pars)
Add row below selected | Delete selected rows
Update model with iterat... | Write iteration model to ...
RESET FIGURE
Exit

giancarlo.bernasconi@polimi.it
gianguido.gentili@polimi.it

Figure 31.Inversion model parameters

2.4.4.6   Inversion Modeling Result

In order to interpret the data from the cruise, I have developed a 1D forward code to compute the response of a layered structure (see Chapter 2 for details). Figure 30 shows the step response of models which has been changed by different frequencies to plot resistivity model of dada, calculated with this code, plotted together with the stacked step response at a sample waypoint from the field data. Model from the figure is the result obtained from a 1D inversion scheme which it has been developed for interpreting the data by Deportment of electronic and information - Politecnico di Milano under supervision of Professor G. Bernasconi. The iterative inversion algorithm calculates the required changes in parameters to minimize the misfit between the forward model and data for a range of parameter step sizes at each iteration. The code is capable of inverting for the conductivity and thickness of a layered structure, water conductivity, TX-RX offset, and water depth and different frequencies.

According to the final calculation which has been approached (see in Figure 30), generally, we can considering that the results from ID inversion scheme are completely tangible to the real model data set of Faroe Island, although, the final result for phase of Ex from frequency of 0.125Hz is not smoothly fit to the real on but the percentage of residual is about less than 0.82% which means negligible.
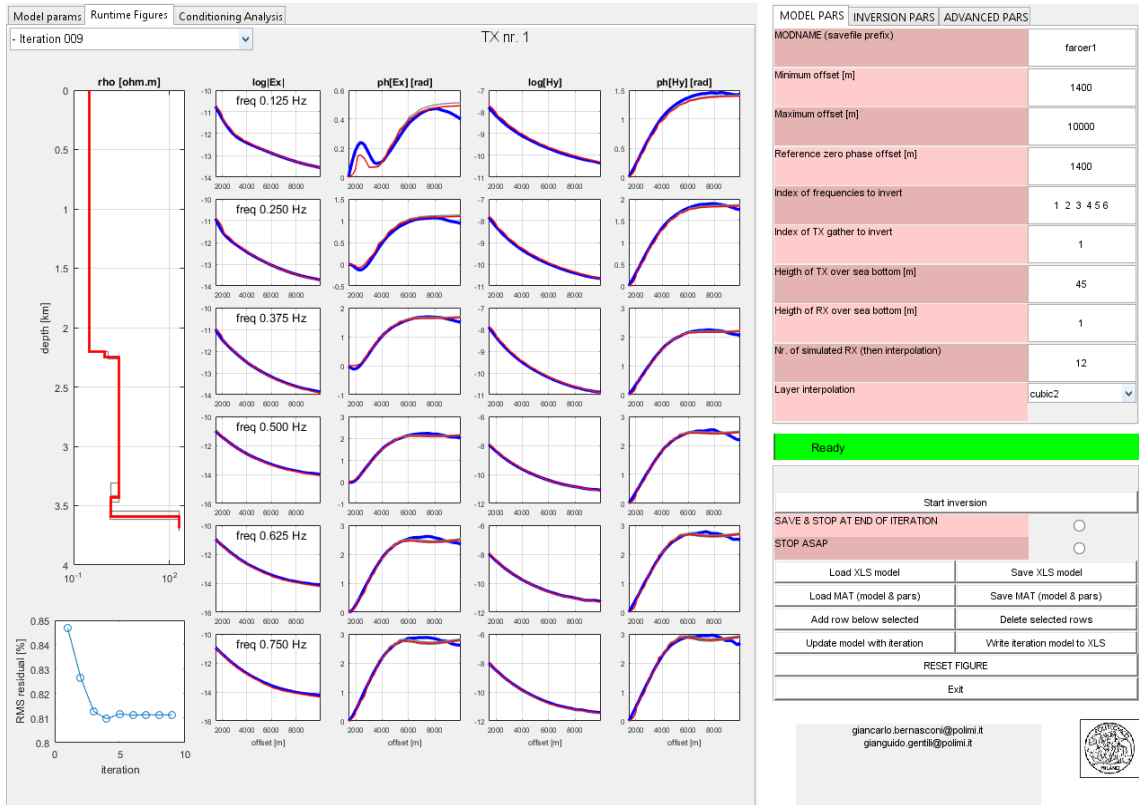
Figure 32. Result of Ex and Hy and Phase and fields for inverted model

For this data set(See table), we have inverted for the resistivity and the transmitter-receiver offset in a half-space model, given the water depth and water conductivity (from Conductivity-Temperature Depth (CTD) measurements in the area) at each waypoint. The results, which are plotted in Figure 31, show that the apparent resistivity in the area is between 1 to 2 Ωm. The inverted values for the TX-RX offset are lower than the theoretical 350 m (middle of RX to middle of TX dipole) by a few percent possibly due to the array not being completely straight and flat on the seafloor.

Depth [m]	Resistivity [Ohm-m]
0	0.3
2200	0.3
2248.216	0.919913
3428.556	2.493567
3587.452	1.384604
3587.452	191.1112

In conclusion, the results of conductivity analysis which has been plotted in figure 31. Presents that thickness and resistivity of layers are acceptable from the real data and we can use 1D inversion modelling for fast interpretation of reservoir characterization.
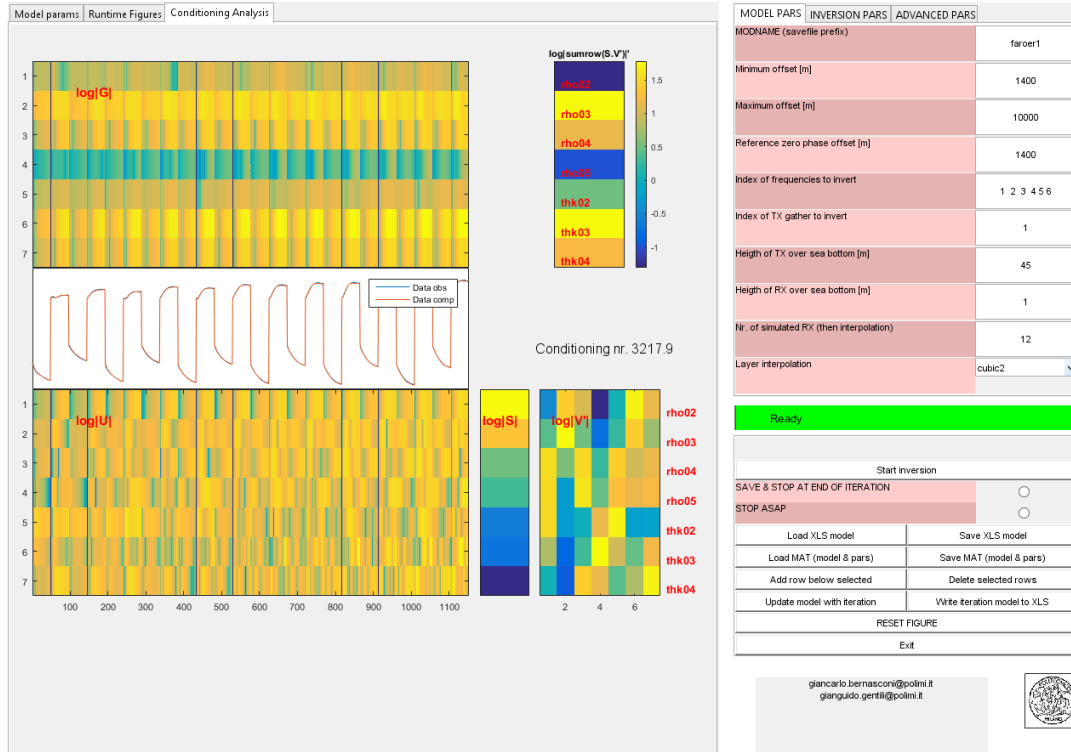
Figure 33. Conductivity Analysis of inversion model

In conclusion, the inversion method recomputed the model parameters according to the real data (Blue Curve) by changing frequencies to up grading the model to reduce the residual percentage.

The inversion algorithm implemented from the theory which was explained in previous section based on the Jacobean matrix Gk of the derivatives of the forward model equation with respect to the current model parameters.

As we can see, low sensitivity is approached with respect to the thickness, for three layers of model we obtained four resistive coefficient (Ohm-m) in Jacobiam Matrix, Gk, which the color bar indicate how the matrix is sensitive with respect to resistivity and thickness of model from receiving data of on receiver.

All in all, the final result indicates how we can control the sensitivity of objects and considering the condition of resistivity model that has been developed.

49

2.5 Sensitivity Analysis of 1D mCSEM modelling

Sensitivity analysis (SA) is widely used in engineering design. One of the widespread SA approaches is based on local methods. Local SA techniques are usually concerned with the computation of the derivative of the model response with respect to the model input parameters. The main disadvantage of these methods is that they do not account for interactions between variables and the local sensitivity coefficients are related to a fixed nominal point in the space of parameters.

The numerical examples are done using simple models and configurations to understand the fundamental behaviour of these modelling methods, for instance how the electric field is changing with frequency, size, depth and thickness. Although in more complex scenarios, different responses for the electric field are expected, the same fundamental behaviour is also expected to be confirmed.

2.5.1 General Introduction

Global SA offers a comprehensive approach to the model analysis. Unlike local SA, global SA methods evaluate the effect of a factor while all other factors are varied as well and thus they account for interactions between variables and do not depend on the choice of a nominal point. Reviews of different global SA methods can be found in [1, 2]. The method of global sensitivity indices suggested by *(Sobol.1990)*, and then further developed by (*Saltelli and Sobol)*, Homma and (*Saltelli 2004)* is one of the most efficient and popular global SA techniques. It belongs to the class of variance-based methods. These methods provide information on the importance of different subsets of input variables to the output variance. Variance- based methods generally require a large number of function evaluations to achieve reasonable convergence and can become impractical for large engineering problems. This is why a number of alternative SA techniques have been proposed recently. One of them is the screening method proposed by Morris [6]. It can be regarded as global as the final measure is obtained by averaging local measures (the elementary effects). This method is considerably cheaper than the variance-based methods in terms of computational time. The Morris method can be used for ranking and identifying unimportant variables. However, the Morris method has two main drawbacks. Firstly, it uses random sampling of points from the fixed grid (levels) for averaging elementary effects, which are calculated as finite differences with the increment delta comparable with the range of uncertainty. For this reason it cannot correctly account for the effects with characteristic dimensions much less than delta. Secondly, it lacks the ability of the Sobol' method to provide information about main effects (contribution of individual variables to uncertainly) and it cannot distinguish between low-and high- order interactions.

In the case of CSEM data, linearization of the inversion procedure would be performed through the Jacobian matrix of sensitivities which contains partial derivatives of the data with respect to the model parameters (Farquharson, 1995).

$$d^{Obs} = A.\,[m] + J[m].\,\partial[m] + e$$

d^{Obs} : Observation data

m: model parameters

A[m]: data equivalent to the defined model

J: Jacobian matrix of sensitivities

∂ [m]: perturbation

e: the remainder

$$J_{ij}[m] = \left.\frac{\partial A_{i[m]}}{\partial m_j}\right.$$

$$i = 1,2,3,\ldots,M$$

$$j = 1,2,3,\ldots,N$$

Where M is the number of observations and N is the number of model parameters *(Farquharson, 1995).*

2.5.2 Sensitivity analysis of 1D CSEM modelling

The numerical examples are done using simple models and configurations to understand the fundamental behaviour of these modelling methods, for instance how the electric field is changing with frequency, size, depth and thickness with respect to different acquisition types (VED, HED and TSEM). Although in more complex scenarios, different responses for the electric field are expected, the same fundamental behaviour is also expected to be confirmed.

For example, in spite of different responses due to different shapes of the reservoir, they will all show the same trend and effect in their responses while moving them in depth, and assuming other parameters unchanged.

In general a simple model as an index can help the interpreter to observe if the change in the electric field is caused by different added complexity to the lithology or that can be due to different size, or depth or different ranges of the frequencies or other parameters.

Generally, the data (models) was explored and processed specifically with the aid of a high performance language for technical computing, the computer Programme MATLAB which has been developed by *department of electronic and information in Poliecnico Di Milano,* especially prof. Gentili. A special processing approach for handling and analyzing marine CSEM data is duly implemented on the models, which has been explained, respectively, following the under listed and explained sequence of steps.

$$E_{tot} = E_1 + E_s = G(J_1) + G(J_s)$$
$$J_s \cong (\sigma_{body} - \sigma_{seabed})E_1$$

Where

E_1 is the primary field (computed with air, sea and seabed)

E_s is the scattered field (computed with air, sea and seabed)

J_s is the induced source (depends on primary field)

G is the Green's function (numerical or analytical)

Is a measure of the strength of the scattered field as a function of scattered position and receiver position a 2D color map represents sensitivity as a function of scattered position for a given receiver position.

2.5.2.1   Sensitivity of response to layer depth

As an example of a layered model, Figure 26 shows a model study in which the response of the inline and vertical dipole array are calculated for a buried layer at varying depths. Sensitivity is calculated as a difference between the response of the layered model and the uniform space. The plots in Figures 27 to 38 shows the sensitivity as a function of depth and offset, according to four frequencies (0.2Hz, 0.48Hz, 0.76Hz and 1.04Hz) to the layers are in see bottom with respect to all mCSEM method (VED, HED and TSEM). Although the layer is close to the seafloor, it is simply too thin to have a significant response. The electric field induced by the transmitter in the resistive layer exits the layer long before arrival at the receiver.

On the sensitivity curve, the layer is far too deep to affect the background response. Here, the electric field arrives at the receiver before interacting with the layer at all.

Sensitivity decreases as the layer moves deeper, and when the depth of the layer reaches the transmitter-receiver offset and beyond, the measurement is no longer sensitive to the presence of the layer.

2.5.2.2   Sensitivity of response to frequencies

In this experiment the integrated sensitivity of the Ex and Ez component were calculated for different frequencies: 0.20Hz, 0.48Hz, 0.76Hz and 1.04Hz (Figures 27 to 38). We can observe in these figures that the higher the frequencies are, the more concentrated and higher sensitivity is in the vicinity of the receiver. The total field strength, however, will decrease with increasing frequency, making the data less robust with respect to ambient noise. As one would expect, the sensitivity decreases faster with the depth and distance from the transmitter when there is an increase in the frequency, which is a simple manifestation of the skin-effect.

2.2.2.3   Sensitivity of response to survey design (offset)

The transmitters generate a frequency domain EM field with a frequency of 0.20 Hz, 0.48Hz, 0.76Hz and 1.04Hz from source point located along the corresponding receiver's line. The maximum and minimum transmitter receiver offsets are 7700 m and 110 m, respectively. The sensitivity analysis of the survey with this condition for three type of acquisitions, have seen that by increasing the offset the derivatives amplitude of Ex and Ez are decrease, the closer the body is to the sea floor, the higher the sensitivity is. (See Figures 27 - 38).
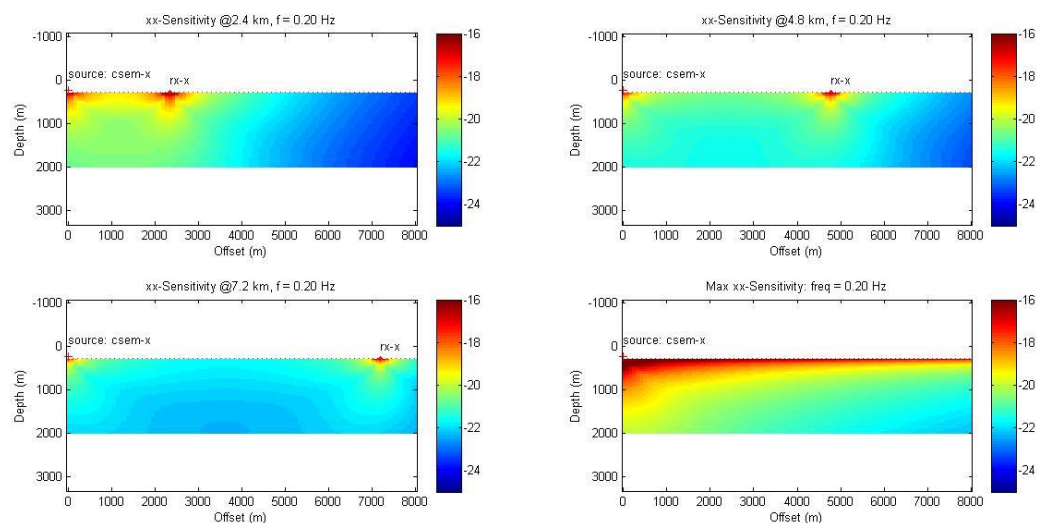

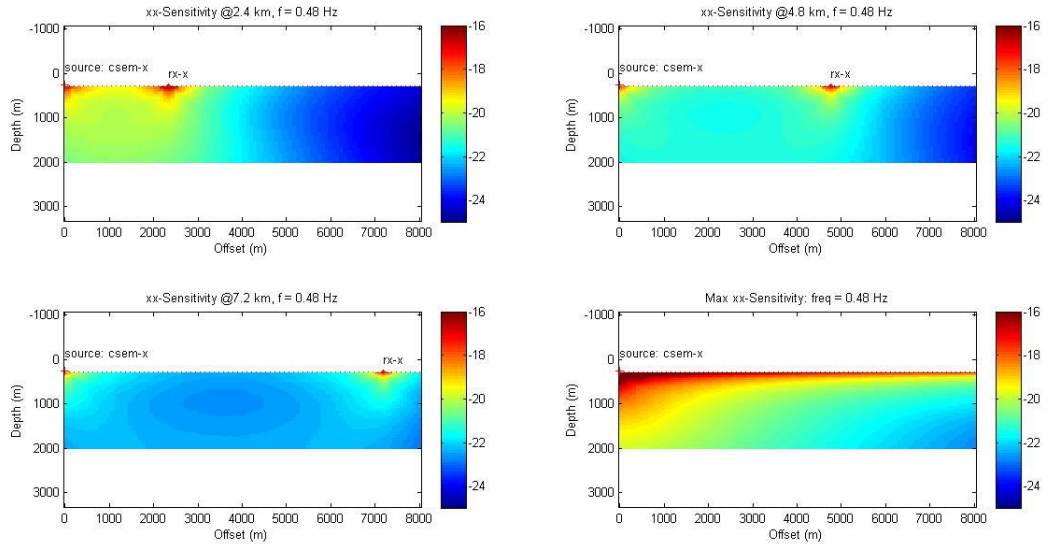*Figure 34. Sensitivity plot of HED with frequency of 0.20Hz*
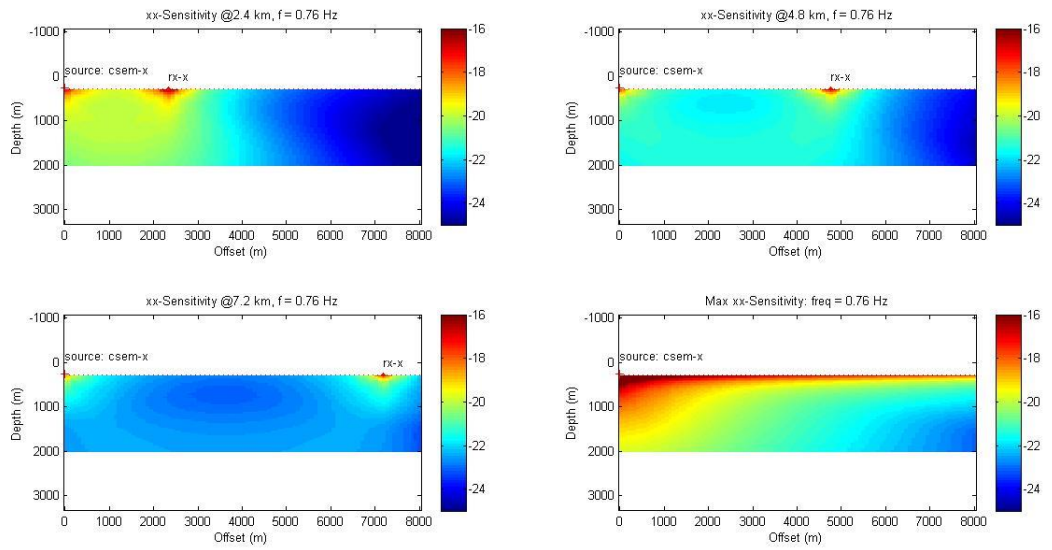
Figure 35. Sensitivity plot of HED with frequency of 0.48Hz

Figure 36. Sensitivity plot of HED with frequency of 0.76Hz
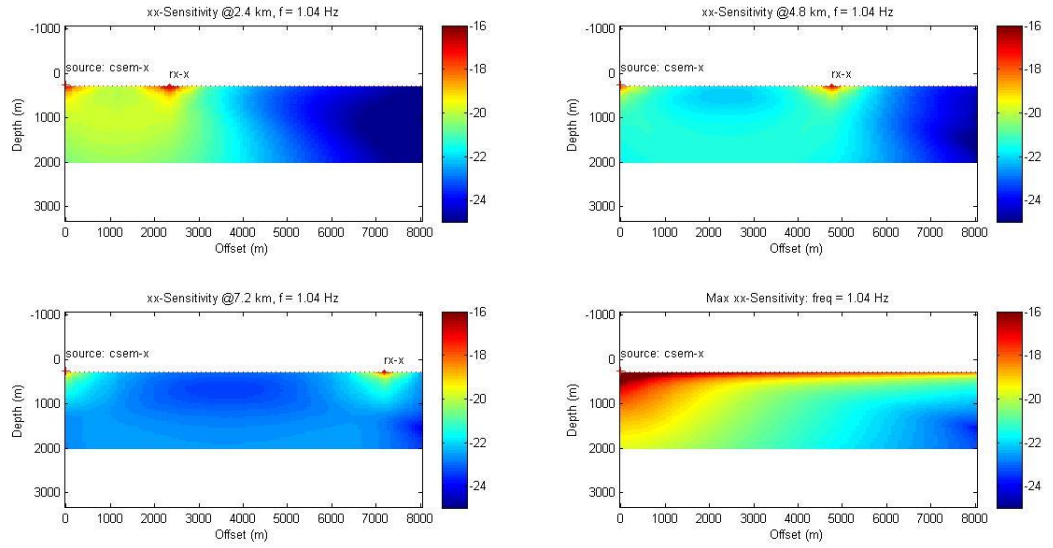
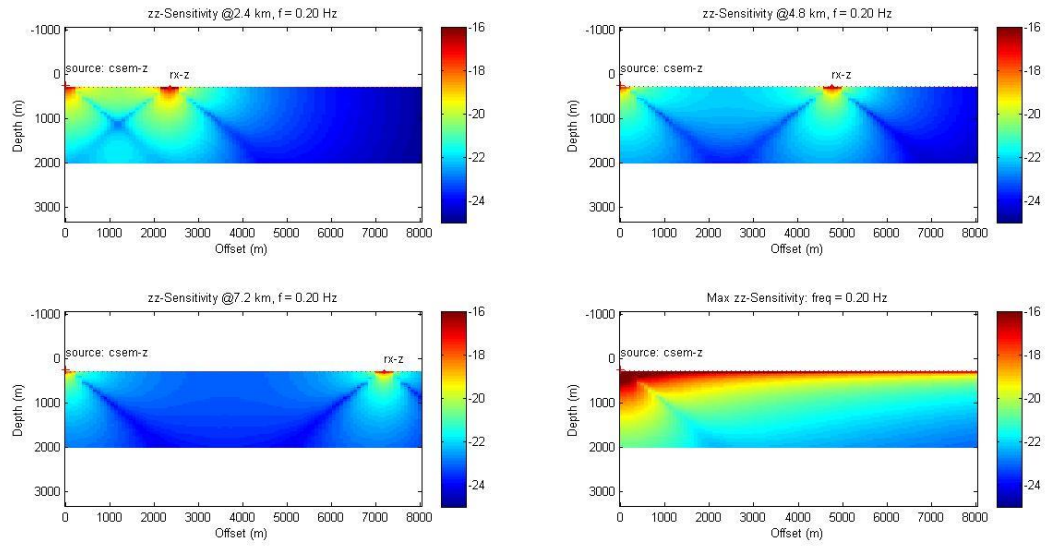*Figure 37. Sensitivity plot of HED with frequency of 1.04Hz*

Figure 38.Sensitivity plot of VED with frequency of 0.20Hz
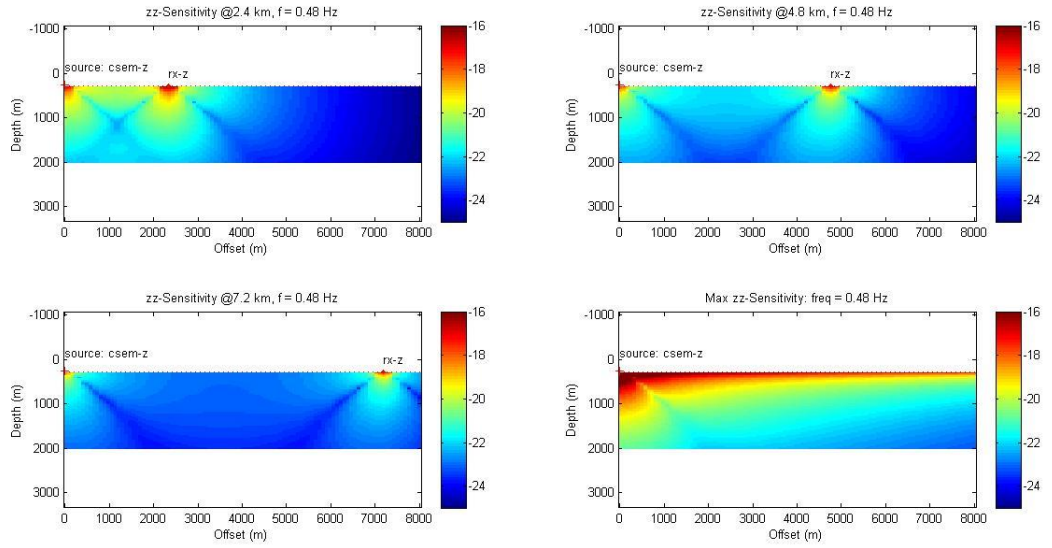
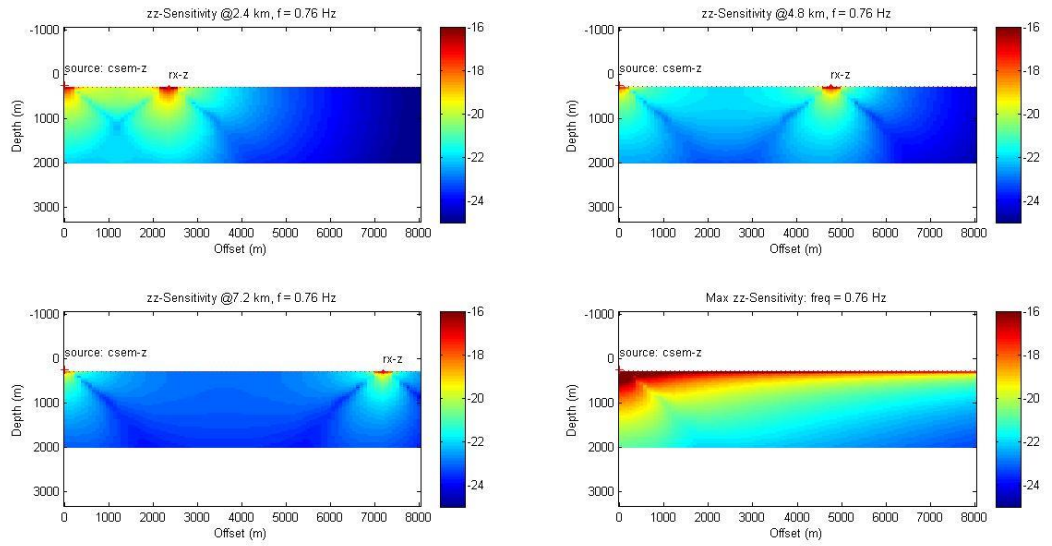*Figure 39..Sensitivity plot of VED with frequency of 0.48Hz*

Figure 40.Sensitivity plot of VED with frequency of 0.76Hz
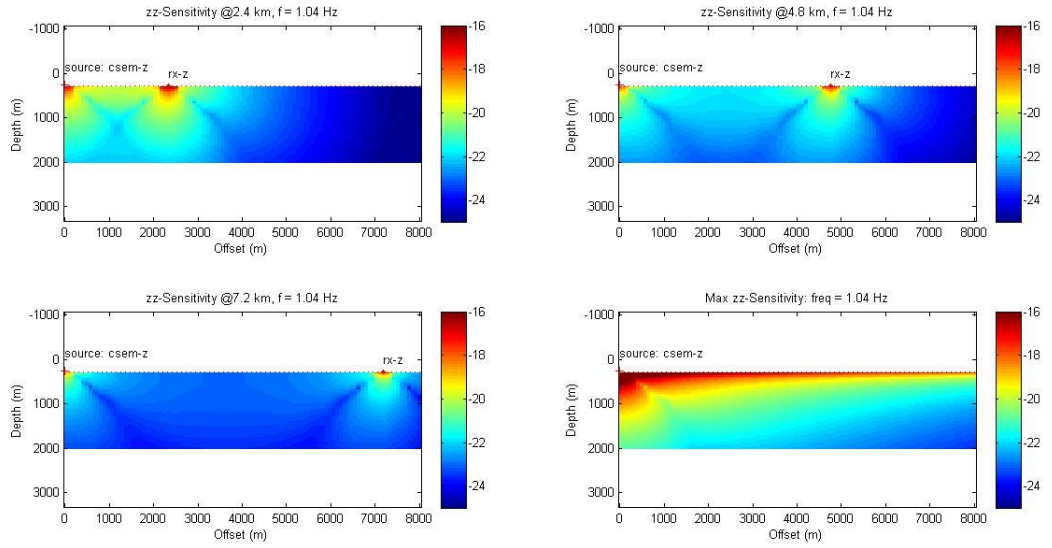
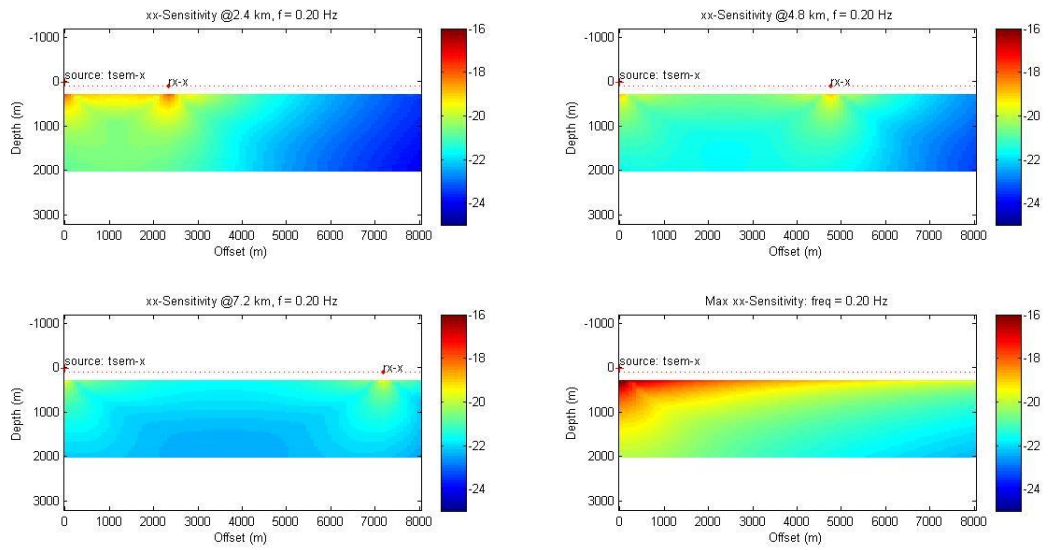*Figure 41.Sensitivity plot of VED with frequency of 1.04Hz*

Figure 42.Sensitivity plot of TSEM with frequency of 0.20Hz
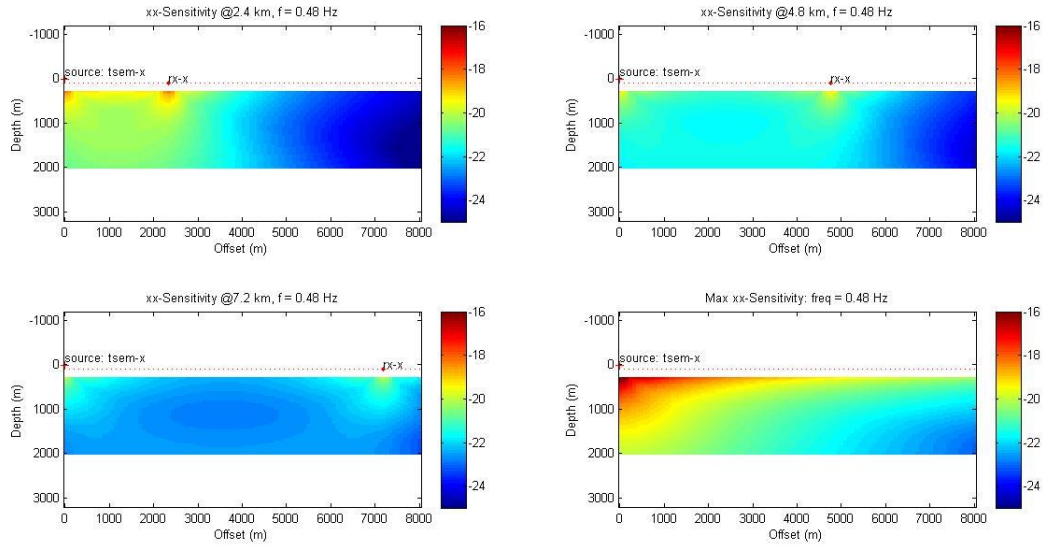
Figure 43.Sensitivity plot of TSEM with frequency of 0.48Hz
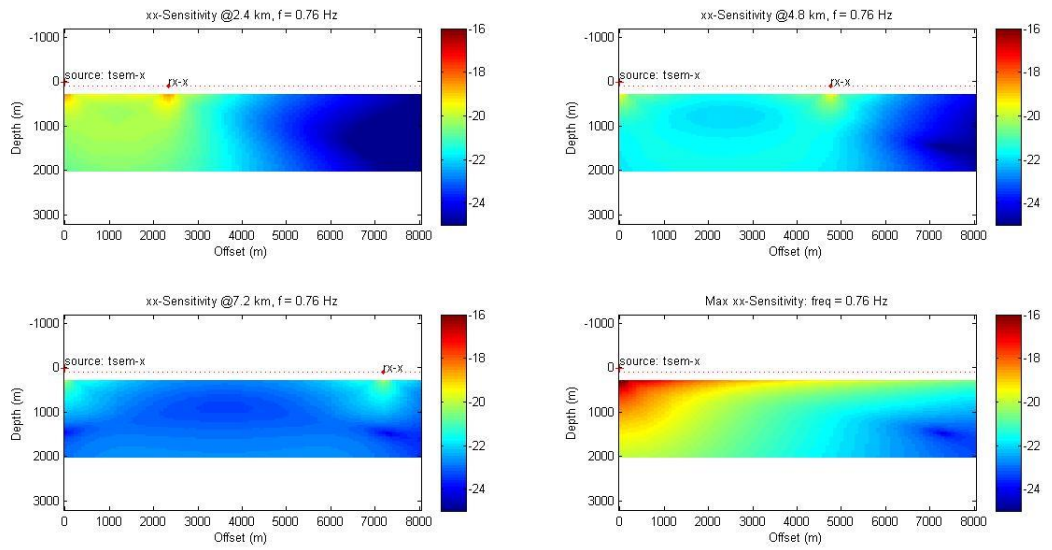
Figure 44.Sensitivity plot of TSEM with frequency of 0.76Hz
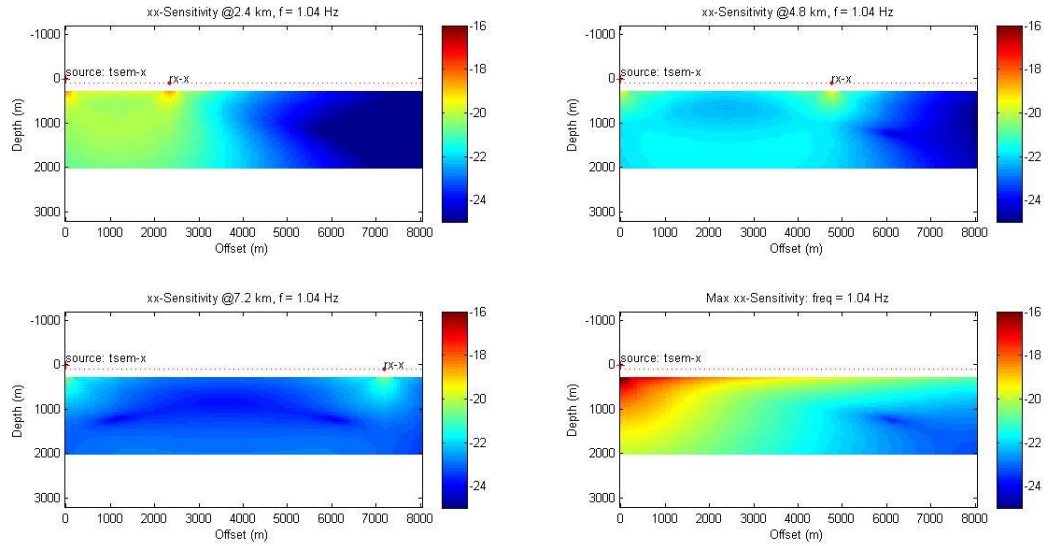
Figure 45.Sensitivity plot of TSEM with frequency of 1.04Hz

We have demonstrated the sensitivity of the model results to several parameters of each CSEM configuration.

In the JxEx method sensitivity benefits from increasing offsets, while at near offsets JzEz benefits from decreasing frequencies, i.e towards the late times. In both methods however, the signal will drop below the background noise floor, in one case from geometrical attenuation of the signal and in the other due to the increasing amplitude of natural fields with decreasing frequency, or in time domain the decay of the fields below the measurement noise.

In conclusion, as we can see in all figures of this chapter we have discovered the feasible area for analysis of sensitivity with respect to HED, VED and TSEM which in next chapter we discuss.

Chapter 3   Conclusion and Discussion

The objectives of this dissertation are elucidated in the introduction. The first objective was to develop sensitivity analysis for three methods for one-dimensional modelling of the marine controlled-source electromagnetic method and accelerate the computation via approximations. The second objective was started with computation of inversion model of three techniques of CSEM by one-dimensional modelling to understanding the importance of sensitivity analysis after modelling in the frequency-domain.

The thesis aims to introduce a simplified model to evaluate the sensitivity for all marine CSEM techniques without utilizing complex analytic and numerical procedures.

In this chapter we reflect on these objectives and give general conclusions and an outlook.

3.1   Discussion

In this study considered sensitivity analysis which plays an important role in diminishing the computing resources by enabling the modeler to focus on the most influential involved factors and eliminate the others problem of inverting CSEM data. Prior to perform the system modelling, the main features of the electromagnetic field propagation in the subsurface are investigated. Several strategies are applied in the regularization the CSEM data for representing the magnitude and phase, of the electric and magnetic field, on the same range scale.

An examination of the sensitivity and resolution of the properties of the canonical model provides a way to compare the all CSEM methods such as explained in the previous section.

The hydrocarbon reservoir always have very low conductivity values compared to its background, thus having negative contrast conductivity (Zhdanov 2009). It has been discussed in chapter 2 how the different parameters affect; (1) the magnitude and phase of the anomalous electric field ; (2) water depth ; (3) depth, resistivity and size of the target and (4) frequency.

3.2   Conclusion

In this paper, we introduce a simple technique of EM data sensitivity analysis based on the reciprocity principle and integrated sensitivity calculations. We have applied this technique to evaluate the sensitivities of the various survey configurations used in MCSEM geophysical methods. We have showed the effects of the frequency of the transmitted EM signal, the different components of EM field, and the number and orientation of the lines in the survey. All these parameters play an important role in determining the overall sensitivity of the observed MCSEM data.

In this experiment the integrated sensitivity of the Ex and Ez components ware calculated for different frequencies: 0.20Hz, 0.48Hz, 0.76Hz, and 1.04Hz (Figures 41 - 43). We can observe in these figures that the higher the frequencies are, the more concentrated and higher sensitivity is in the vicinity of the receiver.
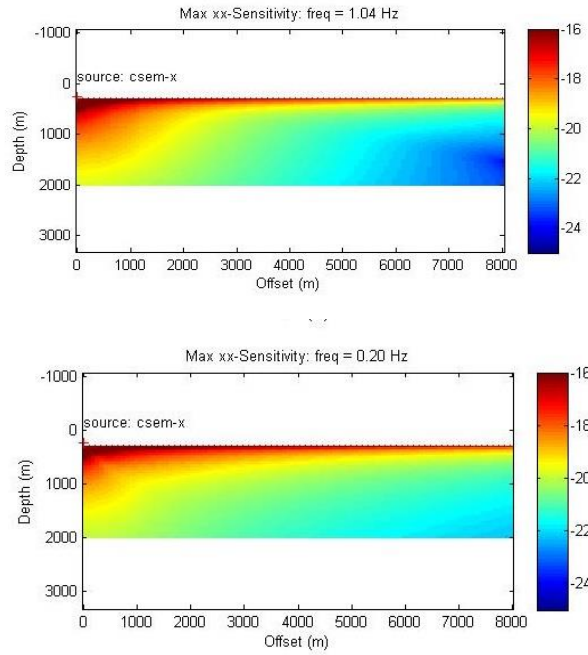
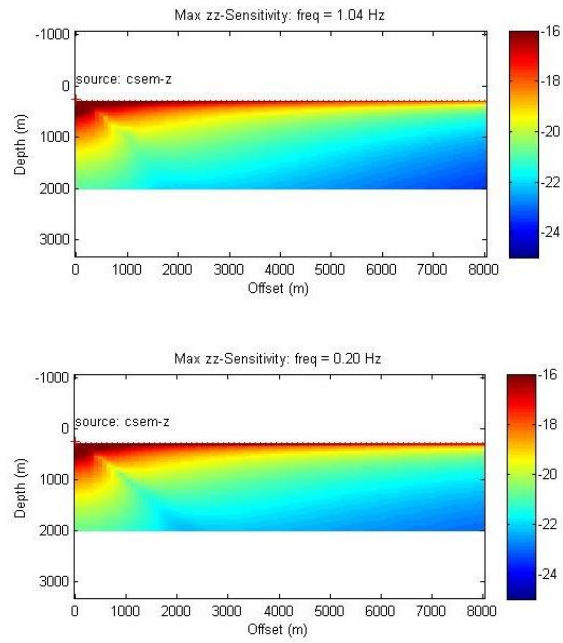*Figure 46. Sensitivity comparison with respect to frequency (HED)*

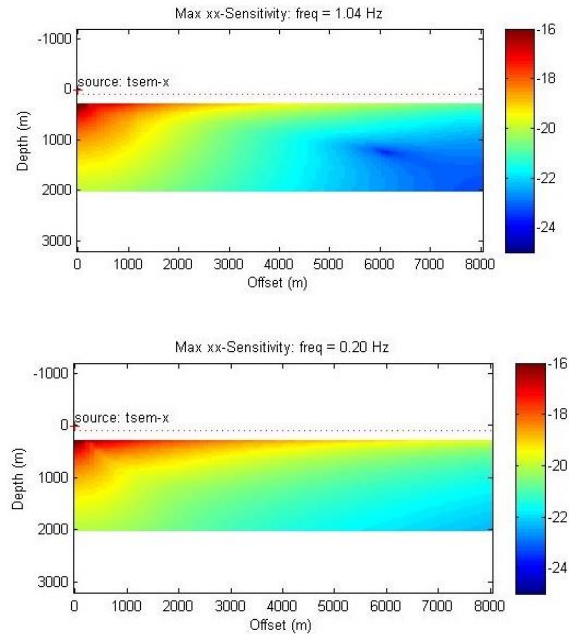*Figure 47.Sensitivity comparison with respect to frequency (VED)*

Figure 48.Sensitivity comparison with respect to frequency (TSEM)

As one would expect, the sensitivity decreases faster with the depth and distance from the transmitter when there is an increase in the frequency, which is a simple manifestation of the skin-effect, according to those plots, we distinguish that for VED the sensitive area is more close to receiver than HED, for instant, at the offset 2000m with the same frequency (0.20 HZ) for VED configuration the sensitive depth is 1000m, although, in HED as we can see, it is more and less 2000m.

In this work a comparison for the sensitivity to the presence of a resistive target of two marine CSEM measurement methods is shown by frequency domain of JxEx and JzEz.

From an analytical perspective it is shown that at far offsets from the source changes in the fields are proportional to the radial distance, for the near offset JzEz instead, sensitivity increases with decreasing frequencies.

Results from comparing the sensitivities of the three type of CSEM configurations (HED, VED and TSEM) Suggest that HED is better suited for the canonical model with high frequency.

We have compared the sensitivities of the marine CSEM method to hydrocarbon-filled layers for the for TSEM, VED and HED sources. The advantage of the deep towing (HED) is that very little EM energy is lost while propagating through the sea water, therefore it is preferred at larger water depths.

The use of the vertical component of the EM field enables improved horizontal resolution compared to conventional EM methods, which are based on horizontal sources and receivers. This vertical

component is also sensitive to deep resistive layers, it avoids interferences by atmospheric noise, the direct wave and the airwave in the underground response.
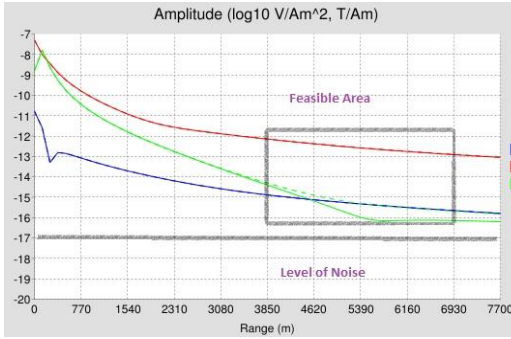

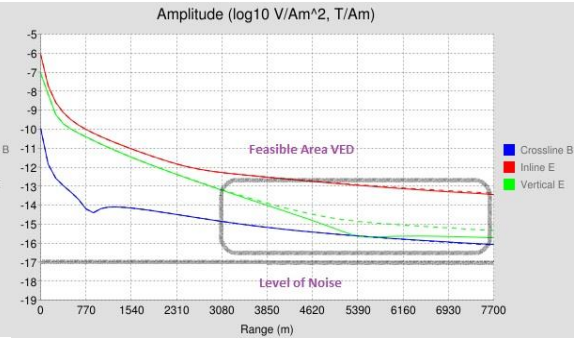Figure 49. Ex layer responded at 0.20Hz (TSEM)
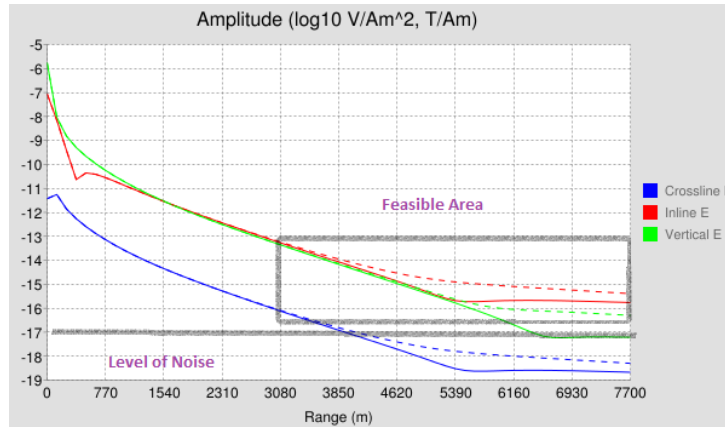
Figure 46. Ez layer responded at 0.20Hz (VED)

Figure 50.Ex layer responded at 0.20Hz (HED)

To prove which method is reliable more than the others we set the noise level at amplitude around 10^{-16} and 10^{-17} V/A.m^2 (figures 44- 46) and as it shows with TSEM acquisition the variation of amplitude based on offset are above the noise level (between 10^-8 and 10^-11) but according to the result it is obvious that this method is not useful for deep target, in order to, with VED acquisition by increasing the offset the variation of amplitude is going to reach the level of noise , at the end as we can see with HED acquisition this limitation for noise level in far offset is acceptable (at offset = 6930m reaches the noise level 10^{-16}) and the feasible area is more clear the others.

In comparison resolution to resistive layer is better obtained at far offsets and using the JxEx measurement, which benefits from the radial falloff of the guided mode phenomena developing at far offsets from the source.

This study shows that the JxEx mode provides better sensitivity and resolution to the presence of wide targets (width À depth). Conversely the JzEz provides better sensitivity as the target's lateral extent becomes comparable and smaller than its depth.

In summary, we conclude that the developed methodology of sensitivity analysis can provide useful information for planning and designing MCSEM surveys for offshore petroleum exploration.

Appendix A

Model, Transmitter and Receiver Geometry

The 1D model uses a right handed Cartesian geometry with the z axis pointing down, as shown in Figure 42. All positions are in units of meters and angles are in degrees. There are N-layers with resistivity ρ in units of ohm-m and each layer position is defined in terms of the top depth of the layer. There are no fixed assumptions of any layer depths, including the air-sea interface. So you will need to describe the entire model in the setup les. Receivers and transmitters can be located anywhere in the stack of layers. When modeling real survey data, you will need to decide what the x; y axes correspond to. For example, you could use UTM coordinates and have x = North, y = East. Or you could have survey local coordinates where x = inline, y = cross line, or y = inline, x = cross line. Whatever you choose, it must be consistent between the transmitters and receivers and the angles defined below. Check and then double check that you've done the correct transformations.
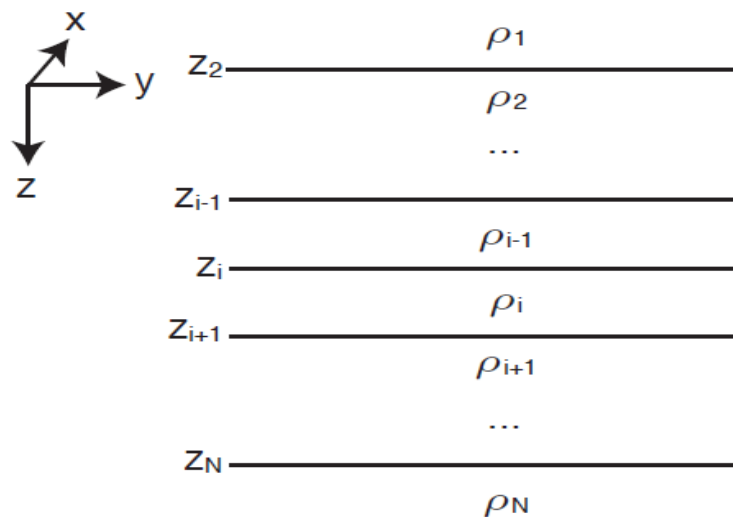
Figure 51. 1D model geometry. There are N-layers with resistivity ρ in units of ohm-m. Each layer is defined in terms of the absolute depth of the top of the layer in units of meters. Receivers and transmitters can be located anywhere in the stack of layers.

CSEM MVO AND PVO PLOTS

Transmitter Orientation

The transmitter orientation parameters are shown in Figure 43. The transmitter azimuth is defined to be the horizontal rotation of the transmitter antenna from the x axis, positive towards y. So an angle of 0 means the antenna points along x, while an angle of 90 degrees means the antenna points along y. If x is also the towline direction, then the azimuth is equivalent to the antenna yaw. The transmitter dip angle is positive down from the azimuth

angle. A dip of 0 degrees means the antenna is horizontal. A dip of 90 degrees means the antenna is pointing downward. If the tail of the antenna is sagging, the dip angle will be negative. If the tail is higher than the head of the antenna, the dip angle will be positive. Dipole1D supports modeling using either a point dipole approximation (faster) or a finite length dipole (slower but more accurate for short range data).

For a finite length antenna, the (x; y; z) position of the antenna should be given as the antenna midpoint. Lastly, note that the term azimuth here refers to the orientation of the antenna, not the source-receiver azimuth used in earlier cylindrical coordinate modeling parameterizations.
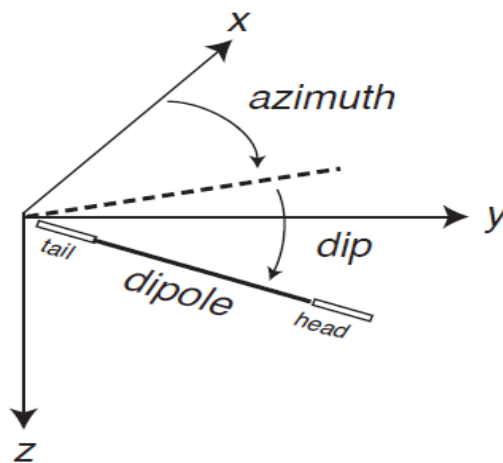
Figure 52. Transmitter orientation parameters. The transmitter azimuth is defined to be the horizontal rotation of the transmitter antenna from the x axis, positive towards y. So an azimuth of 0 means the antenna points along x, while an angle of 90 degrees means the antenna points along y. The transmitter dip angle is positive down from the azimuth angle.

RECEIVER ANGLE CONVENTIONS

A right-hand coordinate system is used with z positive down-wards. All angles are positive clockwise, and receiver azimuth is computed from north to Ex channel.
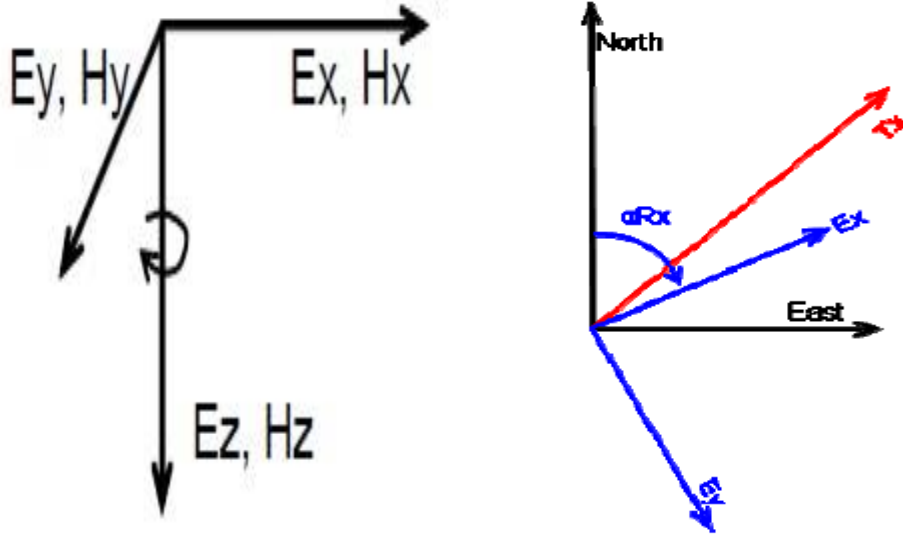
Figure 53. CSEM convention for data processing

Appendix B

POTENTIAL FORMULATION FOR A VERTICAL ELECTRIC DIPOLE

For an electric dipole pointing in the z-direction, the vector potential has the form $\hat{A}$ = (0, 0,$\hat{A}_z$), with Hankel transform expressions

$$A_z(\mathbf{r}) = \frac{1}{2\pi} \int_0^\infty \hat{A}_z(\lambda,z) J_0(\lambda r) \lambda d\lambda,$$

Where $\hat{A}_z$ has the form

$$\hat{A}_{z,i} = c_i e^{\gamma_i(z-z_{i+1})} + d_i e^{-\gamma_i(z-z_i)} + \delta_{ij} \frac{\mu}{2\gamma_j} e^{-\gamma_j|z-z_s|}.$$

By using the recursion for $S_i^\pm$ defined in equation A-8, the potential coefficients in the source layer are found to be

$$d_j = (S_j^+ e^{-\gamma_j|z_{j+1}-z_s|} + e^{-\gamma_j|z_j-z_s|}) \frac{S_j^- e^{\gamma_j h_j}}{1 - S_j^- S_j^+} \frac{\mu}{2\gamma_j}.$$

The coefficients in other layers are found by using either upward or downward continuation of the potential and noting the continuity at layer interfaces.

Bibliography

Alumbaugh, D., N. Cuevas, J. Chen, G. Gao, and J. Brady, 2010, Comparison of sensitivity and resolution with two marine CSEM exploration methods: 80th Annual International Meeting, SEG, Expanded Abstracts, 3893–3897

Albert Tarantola , 2005, Inverse Problem Theory and Methods for Model Parameter Estimation

Anderson, C., and J. Mattsson, 2010, An integrated approach to marine electromagnetic surveying using a towed streamer and source: First Break, 28, 71–75.

Barsukov, P., E. B. Fainberg, and B. Sh. Singer, 2007, A method for hydrocarbon reservoir mapping and apparatus for use when performing the method: Patent WO 2007/053025 A1.

Bension Sh. Singer and Svetlana Atramonova, Vertical electric source in transient marine CSEM: Effect of 3D inhomogeneities on the late time response, GEOPHYSICS, VOL. 78, NO. 4 (JULY-AUGUST 2013); P. E173–E188, 7 FIGS. 10.1190/GEO2012-0316.1

Bhuyian, A., M. Landrø and S. Johansen (2012). "3D CSEM modeling and time-lapse sensitivity analysis for subsurface storage." GEOPHYSICS 77(5): E343-E355.

Constable, S. and L. Srnka "An introduction to marine controlled-source electromagnetic methods for hydrocarbon exploration." GEOPHYSICS 72(2): WA3-WA12.).

Constable SC, Orange AS, Hoversten GM, Morrison HF (1998) Marine magnetotellurics for petroleum exploration part I: a sea-floor equipment system. Geophysics 63(03):816–825

Constable, S. (2010). "Ten years of marine CSEM for hydrocarbon exploration." GEOPHYSICS 75(5): 75A67-75A81.

Constable, S. and C. Weiss (2006). "Mapping thin resistors and hydrocarbons with marine EM methods: Insights from 1D modeling." GEOPHYSICS 71(2): G43-G51.

Cox C (1981) On the electrical-conductivity of the oceanic lithosphere. Phys Earth Planet In 25(3):196–201.

Chave, A. D. and Cox, C. S. [1982] Controlled electromagnetic sources for measuring electrical conductivity beneath the oceans 1. Forward problem and modeling study. J. Geophys. Res., 87, 5327-5338

Engelmark F., Mattsson J. and Linfoot J, 2012, *Simultaneous acquisition of towed EM and 2D seismic – a successful field test, 22nd International Geophysical Conference and Exhibition*

Eidesmo, T., S. Ellingsrud, L.M. MacGregor, S. Constable, M.C. Sinha, S. E. Johansen and F. N. K. a. H. Westerdahl (2002). *"Sea Bed Logging (SBL), a new method for remote and direct identification of hydrocarbon filled layers in deepwater areas." EAGE 20(Vol 20, No 3, March 2002): 9.*

Ellingsrud S, Eidesmo T, Johansen S, Sinha M, MacGregor L, Constable S (2002) *Remote sensing of hydrocarbon layers by seabed logging (SBL): results from a cruise offshore Angola. Lead Edge 21:972–982*

Fabio Marco Miotti, 2012, *"GEOPHYSICAL INVERSION FOR HYDROCARBON RESERVOIR CHARACTERIZATION", Doctoral Dissertation, Politecnico di Milano.*

Flekkoy, E., T. Holten, E. Haland, and K. Maloy, 2010, *extracting the signal from the noise in marine EM measurements: 72nd EAGE Conference and Exhibition, Extended Abstracts.*

Hashin, Z., and Shtrikman, S., 1963, *a variational approach to the theory of the elastic behavior of multiphase materials: Journal of Mechanics of Physical Solids, 11, 127140.*

Jonny Hesthammer a,b,*, Aristofanis Stefatos a, Mikhail Boulaenko a,b, Alexander Vereshagin a, Peter Gelting a, Torolf Wedberg a, Gregor Maxwell a, 2010, *"CSEM technology as a value driver for hydrocarbon exploration", Marine and Petroleum Geology.*

Jon-Mattis Børven , Eirik Grude Flekkøy , 2009, *"Using a vertical dipole source and vertical receivers should increase horizontal resolution of anomalous resistors in offshore EM exploration" , World Oil.*

Kerry W.K. 2003. *Application of Broadband Marine Magnetotelluric Exploration to a 3D Salt Structure and a Fast-Spreading Ridge. PhD dissertation, University of California, San Diego.*

Kerry Key, 2011, *Marine Electromagnetic Studies of Seafloor Resources and Tectonics, Surv Geophys (2012) 33:135–167, DOI 10.1007/s10712-011-9139-x.*

Kang, S., S. J. Seol and J. Byun (2011). *A Feasibility Study of CO_2 Sequestration Monitoring Using the MCSEM Method At a Deep Brine Aquifer In a Shallow Sea.*

Lien, M. and T. Mannseth (2008). "Sensitivity study of marine CSEM data for reservoir production monitoring." GEOPHYSICS 73(4): F151-F163.

Mattsson, J., P. Lindqvist, R. Juhasz, and B. Bjornemo, 2012, Noise reduction and error analysis for a towed streamer EM: 82nd Annual International Meeting, SEG, Expanded Abstracts, doi: 10.1190/segam2012- 0439.1.

Nabighian M.N. and Macnae J.C. 1991. Time Domain Electromagnetic Prospecting Methods.Electromagnetic Methods in Applied Geophysics, ed. Nabighian, M.N., Vol. 2, Society of Exploration Geophysicists, PP427-470.

N. Edwards, 2005, "MARINE CONTROLLED SOURCE ELECTROMAGNETICS: PRINCIPLES, METHODOLOGIES, FUTURE COMMERCIAL APPLICATIONS", Surveys in Geophysics (2005) 26:675–700.

Oldoni M. 2011. Discrete Method for Electromagnetic Modelling - 2.5D electromagnetic simulation for efficient field computation and inverseproblem solving. PhD Minor dissertation, Politecnico di Milano.

P.J. Summerfield, L.S. Gale, X. Lu, T.C. Phillips, R. Quintanilla, 2005, "Marine CSEM Acquisition Challenges" Houston annual meeting SEG 2005.

Ramananjaona, C., L. MacGregor, and D. Andre'is, 2011, Sensitivity and inversion of marine electromagnetic data in a vertically anisotropic stratified earth: Geophysical Prospecting, 59, 341–360, doi: 10.1111/j.1365- 2478.2010.00919.x.

Shahin, A., K. Key, P. Stoffa and R. Tatham (2010). Time‑lapse CSEM analysis of a shaly sandstone simulated by comprehensive petro‑electric modeling. SEG Technical Program Expanded Abstracts 2010: 889-894.

SaltelliA,Tarantola S,Campolongo F,RattoM., Sensitivity analysis in practice.,London: Wiley;2004.

Sobol'I. Sensitivity estimates for nonlinear mathematical models.Matem Modelirovanie1990; 2(1):112–8

S. Kucherenko , M.Rodriguez-Fernandez , C.Pantelides , N.Shah,2008, Monte Carlo evaluation of derivative-based global sensitivity measures, Reliability Engineering and System Safety

S. E. Johansen, H.E.F. Amundsen, T. Røsten, S. Ellingsrud and T. E. a. A. H. Bhuiyan (2005). *"Subsurface hydrocarbons detected by electromagnetic sounding." (Vol 23, No 3, March 2005).*

Scholl C., and R. N. Edwards, 2007, Marine download to seafloor dipole-dipole electromagnetic methods and the resolution of resistive targets: Geophysics 72, 39–49.

Snieder, R. and Trampert, J. 1999. Inverse problems in geophysics (pp. 119-190). Vienna : Springer.

Schön J.H. 1996. Physical Properties of Rocks: Fundamentals and Principles of Petrophysics. Pergamon Press. ISBN 10008044346X.

Swift, C. M. "Fundamentals of the electromagnetic method: Electromagnetics in Applied Geophysics." SEG, 1991: 5-10.

Spies B.R. and Frischknecht F.C. 1991. Electromagnetic Sounding. Electromagnetic Methods in Applied Geophysics, ed. Nabighian, M.N., Vol. 2, Society of Exploration Geophysicists, PP285-417.

S. Marzi, G.Bernasconi, 2014. "Towards Marine Controlled Source EM (M-CSEM) data inversion: sensitivity analysis", Master Dissertation, Politecnico di Milano

Scholl, C., and R. Edwards, 2007, Marine downhole to seafloor dipoledipole electromagnetic methods and the resolution of resistive targets: Geophysics, 72, no. 2, WA39–WA49, doi: 10.1190/1.2434775.

Terje Holten*, Eirik Grude Flekkøy, Knut Jørgen Måløy, and Bension Singer , 2009 , Vertical source and receiver CSEM method in time-domain, SEG Houston 2009 International Exposition and Annual Meeting.

Treite, Svenl and Lines, Laurence R. 1999. Past, present and future of geophysical inversion – a Y2K. s.l. : CREWES Research Report ,Vol. 11.

Terje Holten, Eirik Grude Flekkøy, Bension Singer, Erik Mårten Blixt, Alfred Hanssen, Simultaneous acquisition of towed EM and 2D seismic – a successful field test

Torres-Verdin, C. and T. M. Habashy (1995). "A two-step linear inversion of two-dimensional electrical conductivity." Antennas and Propagation, IEEE Transactions on 43(4): 405-415.

Um, E., and D. Alumbaugh, 2007, on the physics of the marine controlledsource electromagnetic method: Geophysics, 72, no. 2, WA13–WA26.

Um, E., J. Harris, and D. Alumbaugh, 2010, 3D time-domain simulation of electromagnetic diffusion phenomena: A finite-element electricfield approach: Geophysics, 75, no. 4, F115–F126, doi: 10.1190/1 .3473694.

Ward, S. H., and Hohmann, G. W. 1987: Electromagnetic Methods in Applied Geophysics, volume 1 of Investigations in Geophysics, chapter 4 Electromagnetic Theory for Geophysical Applications. Society of Exploration Geophysicists.

Wang, Y., W. Luo, Z. He, W. Sun and Z. Wang (2008). Born Approximation Inversion For the Marine CSEM Data Set.

Zhdanov, M. S. (2009). Geophysical Electromagnetic Theory and Methods. Methods in Geochemistry and Geophysics. Amesterdam, Elsevier. 43.

Zhdanov, M. S. (2002). "Geophysical Inverse Theory and Regularization Problems." Elsever 36: 3-609

Zonge, K. L. and Hughes L.J. 1991. Controlled source audio-frequency magnetotellurics. Electromagnetic Methods in Applied Geophysics, ed. Nabighian, M.N., Vol. 2, Society of Exploration Geophysicists, PP713-809.